Marina V. Rodnina · Wolfgang Wintermeyer
Rachel Green *Editors*

Ribosomes

Structure, Function, and Dynamics

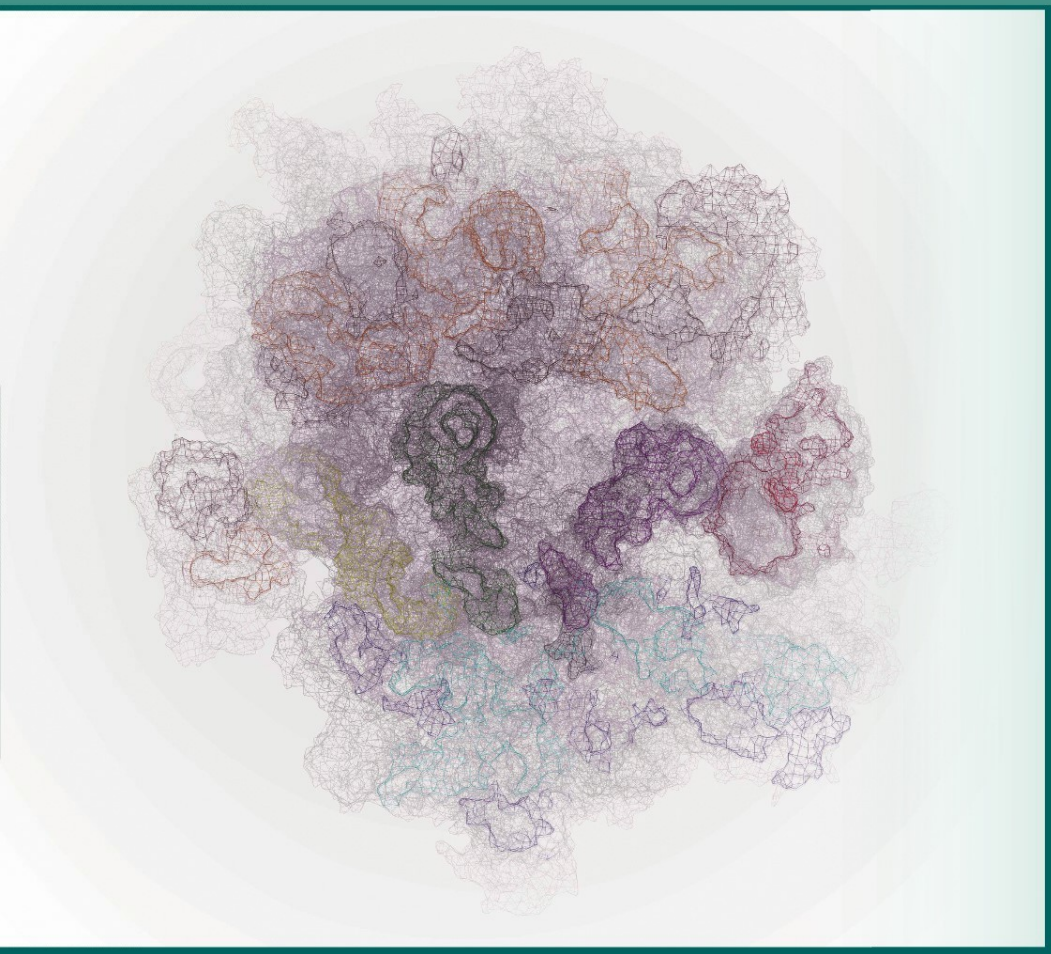

SpringerWienNewYork

SpringerWienNewYork

Marina V. Rodnina
Wolfgang Wintermeyer
Rachel Green
Editors

Ribosomes

Structure, Function, and Dynamics

SpringerWienNewYork

Prof. Dr. Marina Rodnina
Prof. Dr. Wolfgang Wintermeyer
Dept. of Physical Biochemistry, MPI for Biophysical Chemistry,
Goettingen, Germany

Prof. Dr. Rachel Green
Dept. of Molecular Biology and Genetics
Howard Hughes Medical Institute,
Johns Hopkins University School of Medicine, Baltimore, MD, USA

SpringerWienNewYork is part of Springer Science+Business Media
springer.at

Coverdesign: WMX Design GmbH, 69126 Heidelberg, Germany
Layout and Typesetting: JungCrossmedia Publishing GmbH, 35633 Lahnau, Germany
Printing: Holzhausen Druck GmbH, 1140 Wien, Austria

Printed on acid-free and clorine-free bleached paper

SPIN: 80011232

Library of Congress Control Number: 2011928714

ISBN 978-3-7091-0214-5 SpringerWienNewYork

Preface

The breakthrough discovery through which ribosome research entered a new era was the determination, in 2000, of high-resolution crystal structures of subunits of the ribosome, an achievement honored with the Nobel Prize in Chemistry 2009 for Ada Yonath, Tom Steitz, and Venki Ramakrishnan. The articles of this book present research covering about one decade, since the last such book, "The Ribosome", which was published in 2001 associated with a Cold Spring Harbor Symposium series of lectures. The articles are based on presentations given at the meeting "Ribosomes 2010" which was held in Orvieto, Italy, May 3 to 7, and brought together 320 scientists from all areas of ribosome research. Not included in the book are articles about recoding, as the topic was covered very recently in the 2010 book "Recoding" from this same series.

In the first section of this book, new structures of functional complexes of bacterial ribosomes are presented, with an early look at the first crystal structure of a eukaryotic (yeast) ribosome. Next follow chapters focused on structural insights into translation initiation, ribosome recycling, and polysome structure. Subsequent sections deal with mechanisms of decoding, including fidelity, and the chemistry of catalysis in the peptidyl transferase center. In the next section are a number of chapters where the recurrent theme is the structural dynamics of the ribosome. Single-molecule fluorescence methods on the one hand and single-particle cryo-electron microscopic image reconstruction on the other reveal a highly dynamic picture of the ribosome, exhibiting the energy landscape of a processive Brownian machine. The fate of the nascent peptide emerging through the exit tunnel of the ribosome and its interactions inside and outside the tunnel is described in a number of articles. A final chapter on the evolution of ribosomes presents a molecular paleontology approach suggesting how a small, relatively simple primordial RNA molecule may have evolved to become the large and complex structure that we know as the modern day ribosome.

The editors would like to express their gratitude to the authors for their cooperation in preparing their chapters and for providing the basis for a comprehensive overview of ribosome research as of 2010. We hope that the book, as previous "ribosome books", will for a long time serve as a source of information for researchers in the field and for those who are interested in entering this field which becomes ever more fascinating.

Göttingen and Baltimore, June 2011

Marina V. Rodnina
Wolfgang Wintermeyer
Rachel Green

Contents

Section I Ribosome structure

Ribosome crystallography: From early evolution to contemporary medical insights

1

Anat Bashan and Ada Yonath

1. Introduction

Ribosome research took off as soon as ribosomes were identified. At the end of the seventies the extensive biochemical studies yielded illuminating findings about the overall nature of ribosome function. These studies showed that all ribosomes are composed of two unequal subunits. The small subunit in bacteria, denoted as 30S, contains an RNA chain (16S) of about 1500 nucleotides and 20–21 different proteins, whereas the large subunit, denoted as 50S, contains two RNA chains (23S and 5S RNA) of about 3000 nucleotides in total, and 31–35 different proteins. In all organisms the two subunits exist independently and associate to form functionally active ribosomes.

The substrates engaged in protein formation are aminoacylated, peptidylated and deacylated (exiting) tRNA molecules. The three-dimensional structures of all tRNA molecules from all living cells across evolution are alike, although each of them has features specific to its cognate amino acid. The tRNAs are double helical L-shaped RNA molecules in a stem-elbow-stem organization, and contain a loop that comprises the anticodon complementing the three-nucleotide codon on the mRNA. About 70 Å away, at their 3' end, tRNAs contain a single strand with the universal sequence CCA, to which the cognate amino acid is attached by an ester bond. The tRNA molecules are non-ribosomal entities that bring together the two subunits, as all three of their binding sites, A (aminoacyl), P (peptidyl), and E (exit), reside on both subunits. The small subunit provides the path along which the mRNA progresses, the decoding center and the mechanism controlling translation fidelity, and the large subunit contains the site for the main ribosomal catalytic function, namely the polymerization of amino acids.

Although an overall description of protein biosynthesis was available by the end of the seventies, detailed functional information was not available because of the lack of three-dimensional molecular structures. Indeed, the common hypotheses about the mode of ribosome function underwent significant alterations once three-dimensional structures became available. Striking examples for conceptual revolutions in the understanding of ribosomal function (Wekselman et al., 2008) relate to the functional contribution of the different ribosomal components and the path taken by nascent chains.

In the middle of the last century, RNA-rich particles, called "Palade particles", were identified in the vicinity of the endoplasmic reticulum (Palade, 1955; Watson, 1963). These were proposed to be involved in gene expression, suggesting that proteins are made by an RNA machine (Crick, 1968). Nevertheless, it was commonly assumed for over four decades that decoding of the genetic code and peptide bond formation are performed by r-proteins, while r-RNA provides the ribosomal scaffold (Garrett and Wittmann, 1973). The proposition that RNA provides the ribosome catalytic activities (Noller et al., 1992) was met first with skepticism. Modest acceptance of this idea was achieved as several functional roles played by RNA molecules in various life processes were identified around the last decade of the 20th century, including peptide bond formation *in vitro* by selected ribozymes (Zhang and Cech, 1997) and spontaneous conjugation of amino acids with oligonucleotides (Illangasekare et al., 1995). Finally, at the turn of the third millennium, the emerging high-resolution structures verified the notion that both the decoding center and the site of peptide bond formation (called peptidyl transferase center or PTC) reside in regions where rRNA predominates.

The three-dimensional crystal structures of ribosomes and their various complexes illuminated the molecular basis for most of the mechanisms involved in ribosome function. These showed how the assembly of the initiation complex occurs (Simonetti et al., 2008; Simonetti et al., 2009), revealed the decoding mechanism (reviewed in (Ramakrishnan, 2008; Demeshkina et al., 2010)), the mRNA progression mode, including the narrowing of the downstream mRNA tunnel that occurs upon the transition from initiation to elongation (Yusupova et al., 2006; Jenner et al., 2010), identified the relative positions of A-, P- and E-site tRNAs (Yusupov et al., 2001) and shed light on the way the initiation, elongation, termination, and recycling factors modulate ribosome function (Carter et al., 2001; Pioletti et al., 2001; Wilson et al., 2005; Borovinskaya et al., 2007; Laurberg et al., 2008; Weixlbaumer et al., 2008; Schmeing et al., 2009). In addition, the positions of the tRNA molecules within the PTC (Woolhead et al., 2004; Blaha et al., 2009; Voorhees et al., 2009), the conformational rearrangements that E-site tRNA undergoes while exiting the ribosome (Jenner et al., 2007), and the architectural and dynamic elements required for amino acid polymerization were determined (Bashan et al., 2003a; Bashan and Yonath, 2008b). Thus, it appears that the main catalytic activities of the ribosome provide the framework for proper positioning of all participants in the protein biosynthetic process, thus enabling decoding, successive peptide bond formation and the protection of the nascent protein chains.

This article focuses on ribosome crystallography and on the functional implications evolving from these studies. It describes snapshots from the chronological progress of ribosomal crystallography as a semi historical report. It highlights selected events occurring during the long way from the initial ribosome crystallization including the introduction of innovations in the procedures required for the determination of the ribosomal structures, such as cryo bio-crystallography and the use of heavy atom clusters [reviewed in (Gluehmann et al., 2001)]. The article also focuses on selected structural and dynamic properties of the ribosome that enable its function as an efficient machine and illuminates several key ribosomal strategies for efficient usage of resources and for minimizing protein production under non-optimal conditions. Additionally, this article discusses modes of action of antibiotics that hamper ribosome function and suggests mechanisms for the acquisition of antibiotic resistance. It also addresses issues concerning the origin of translation, as can be deduced from the universal structural element that embraces the ribosomal active site and possesses internal symmetry within the otherwise asymmetric contemporary ribosome.

2. Hibernating bears stimulated ribosome crystallization

Once it was found that ribosomes are the molecular machines translating the genetic code and initial knowledge of the chemical composition of the *E. coli* ribosome became partially available, attempts at ribosome crystallization were made worldwide. For over two decades these attempts were unproductive. Owing to repeated failures the crystallization of ribosomes was considered a formidable task. The extreme difficulties in ribosome crystallization stemmed from their marked tendency to deteriorate, their high degree of internal mobility, their flexibility, their functional heterogeneity, their chemical complexity, their large size and their asymmetric nature.

Nevertheless, the finding that large amounts of ribosomes in hibernating bears are packed in an orderly fashion on the inner side of their cell membranes indicated that ribosomes can assemble in periodical arrangements *in vivo*. Similar observations were made in shock-cooled fertilized eggs (Unwin and Taddei, 1977; Milligan and Unwin, 1986). These phenomena were associated with cold or similar shocks, and were rationalized as a strategy taken by organisms under stress for storing pools of functionally active ribosomes that can be utilized when the stressful conditions are removed. Indeed, structural studies, performed on samples obtained from shock-cooled fertilized eggs led later to the visualization of ribosomal internal features (Milligan and Unwin, 1986) (see below).

Extending the level of order from membrane-supported two-dimensional monolayers produced *in vivo* to three-dimensional crystals grown *in vitro* was not trivial, but became successful with the introduction of uncommon crystallization strategies. These were based on the interpretation of the life cycle of the winter sleeping bears, which regularly pack and unpack their ribosomes each year, as part of their normal life cycle. The fact that these processes are associated with living organisms that require functionally active ribosomes immediately when awaking from a state of winter sleep suggested (i) that the integrity of highly active ribosomes can be maintained for relatively long periods without undergoing significant deterioration and (ii)

that the ribosomes can be periodically ordered in three-dimensions. In other words, ribosomes seemed likely to form crystals.

The breakthrough in ribosome crystallization was based on the assumption that the higher the sample homogeneity, the better the crystals, and secondly, that the preferred conformation is that of the functionally active ribosome. Consequently, highly active ribosomes of bacterial species that grow under robust conditions were selected and conditions for optimization and maintenance of their activity (Vogel et al., 1970; Zamir et al., 1971) were maintained throughout purification and crystallization. The first three-dimensional micro-crystals of ribosomal particles, treated as "powder samples" diffracted to relatively high resolution (3.5 Å) and had impressive internal order (Figure 1), were obtained from the large ribosomal subunit of a thermophilic bacterium, *Bacillus stearothermophilus* (B50S), at the beginning of the eighties (Yonath et al., 1980). A thorough screening of about 25,000 different crystallization conditions, performed by careful monitoring of the nucleation of crystalline region (Yonath et al., 1982a), was accompanied by a systematic search for parameters favoring crystallization (Yonath et al., 1982b). At the beginning of the eighties, *B. stearothermophilus* as an extremophile was considered to be exotic. Therefore frequent doubts about its suitability as a representative of "normal" bacterial ribosomes, such as those of *E. coli*, were expressed, despite the very high sequence homology between them. Nevertheless, the preliminary successes of the crystallization stimulated the use of ribosomes from other robust bacteria. Consequently, a few years later, three-dimensional crystals were obtained from the large ribosomal subunits of the halophilic archaeon, *Haloarcula marismortui*, that lives in the Dead Sea (Shevack et al., 1985). In 1987, seven years after the first crystallization of the large ribosomal subunits, parallel efforts led to the growth of crystals of the small ribosomal subunit (Yonath et al., 1988; Yusupov et al., 1988) and of the 70S ribosome (Trakhanov et al., 1987) from the extreme thermophilic bacterium, *Thermus thermophilus*.

At that time it was widely assumed that the three-dimensional structure of the ribosome may never be determined, as it was clear that alongside the improvement of the crystals, the determination of the structure would require the introduction and development of innovative methodologies. For instance, because of the weak diffraction power of the ribosome crystals even the most advanced rotating anode generators were not powerful enough to yield suitable diffraction patterns. Similarly, only a few diffraction spots could be recorded (Yonath et al., 1984) (Figure 1), even when irradiating extremely large crystals (~2 mm in length) by synchrotron radiation, which at the time was in its early stage. In parallel to the advances in growing ribosomal crystals of several forms (Yonath and Wittmann, 1988), the synchrotron facilities and the detection methods underwent constant (albeit rather slow) improvement. However, even when more suitable beamlines became available, the radiation sensitivity of the ribosomal crystals caused extremely fast crystal decay. Hence, pioneering data collection at cryogenic temperature (Hope et al., 1989) became crucial. Once established, this method became routine worldwide, and, although when using very bright X-ray beam, decay was observed even at cryo-temperature, interpretable diffraction patterns were ultimately obtained from the extremely thin crystals. Additionally, multi-heavy atom clusters suitable for phasing were identified (Thygesen et al., 1996). One of these clusters, originally used for providing anomalous phasing power, was found to play a dual role in the determination of the structure of the small ribosomal subunit from *T. thermophilus* (T30S). Post-crystallization treatment with minute amounts of these clusters dramatically increased the resolution from the initial 7–9 Å to 3 Å (Schluenzen et al., 2000), presumably by minimizing the internal flexibility of the particle (Bashan and Yonath, 2008a).

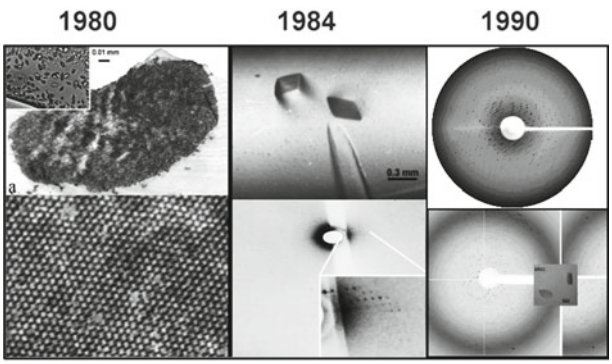

Fig. 1 From micro-crystals to three-dimensional crystals yielding useful diffraction. Left, top: The first microcrystals of B50S (Yonath at al., 1980). Left, bottom: a negatively stained section of the microcrystals, viewed by electron microscopy. Middle, top: the tip of a ~2 mm-long crystal of B50S. Middle, bottom: its diffraction pattern, obtained at 4°C in 1984 using the EMBL/DESY/Hamburg beam line. Right, top: The diffraction pattern from crystals of H50S, obtained at ID13 beamline at ESRF, Grenoble, at 95K; the diffraction extends to 2.8Å. Right, bottom: The crystals decayed completely after collecting about 0.3% of the data.

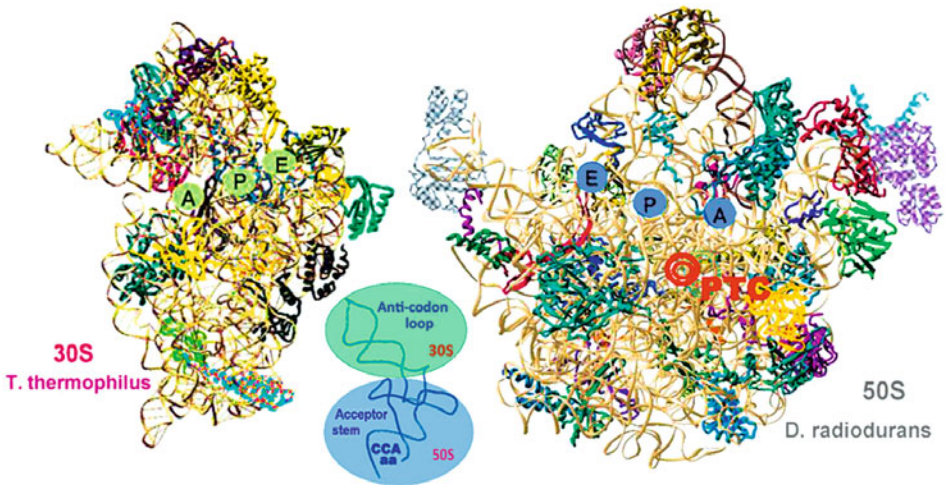

Fig. 2 The three-dimensional structures of the two ribosomal subunits from the bacteria *Deinococcus radiodurans* and *T. thermophilus*. The interface faces are facing the reader. The rRNA is shown in brownish colors, and each of the r-proteins is painted in a different color. The approximate site of the PTC is marked in red. Insert: the backbone of a tRNA molecule. The circles designate the regions interacting with each of the ribosomal subunits.

Continuous efforts were aimed at improving crystals, including the assessment of the influence of the relative concentrations of mono- and divalent ions (von Bohlen et al., 1991) on crystal properties. These efforts led to dramatic improvements in the quality of the crystals of the large ribosomal subunits from *H. marismortui* (H50S). In addition, constant refinements of bacterial growth protocols (Auerbach-Nevo et al., 2005) alongside a thorough investigation of crystallization conditions (Zimmerman and Yonath, 2009), indicated a noteworthy correlation between the conditions at which the ribosome functions and the crystal quality. Along these lines it is worth mentioning that flexible ribosomal regions were detected in electron-density maps obtained from crystals of ribosomal particles that were obtained under conditions that supported optimal functional activity (Harms et al., 2001), whereas the same regions were significantly more disordered in crystals obtained under non-physiological conditions (Ban et al., 2000).

An alternative strategy for improvement of crystal quality was the crystallization of complexes of ribosomes with substrates, inhibitors and/or factors, presumably because these factors trap the ribosomal particles in preferred conformations. Indeed, the initial diffracting crystals of the 70S ribosome from *T. thermophilus* (T70S) with mRNA and tRNA molecules (Hansen et al., 1990) a decade later led to impressive advances in resolution from crystals of functional ribosome complexes (Yusupov et al., 2001; Korostelev et al., 2006b). Importantly, these techniques also enabled the structural analysis of snapshots of ribosomes trapped in specific conformations, albeit not necessarily functional ones (Schuwirth et al., 2005).

3. The ribosome is a polymerase

The crystal structures of bacterial ribosomes showed that the interface surfaces of both ribosomal subunits and their active sites (the decoding center and the peptidyl transferase center) are rich in RNA (Figure 2). These observations verified previous biochemical suggestions that the ribosome is a ribozyme. Particularly, as seen below, the striking architecture of the ribosome governs all tasks related to nascent protein elongation: namely the formation of peptide bonds, the processivity of this reaction, and the detachment of the growing polypeptide chain from the P-site tRNA. Thus, in addition to factor-assisted movements, i. e. the entrance and exit of the tRNA molecules and the progression of the mRNA, amino acid polymerization requires several major motions including peptidyl-tRNA translocation from the A to the P site, entry of the growing chain into the ribosome exit tunnel (Figure 3), passage of the deacylated tRNA molecule from the P to the E site and its subsequent release. However, it should be kept in mind that, although single peptide bonds can be produced by mixtures containing mainly rRNA and traces of r-proteins (Noller et al., 1992), the production

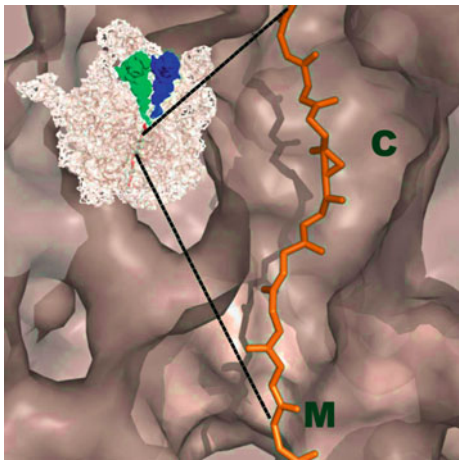

Fig. 3 The ribosomal exit tunnel. The entire large subunit, viewed from its interface surface with A- and P-site tRNAs (blue and green, respectively) and with polyalanine (orange) modeled in the tunnel, is shown in the top left panel. The main view is a zoom into the upper end of the tunnel. C denotes a crevice where co-translational initial folding may occur (Amit et al., 2005), and M shows the tunnel constriction, add.

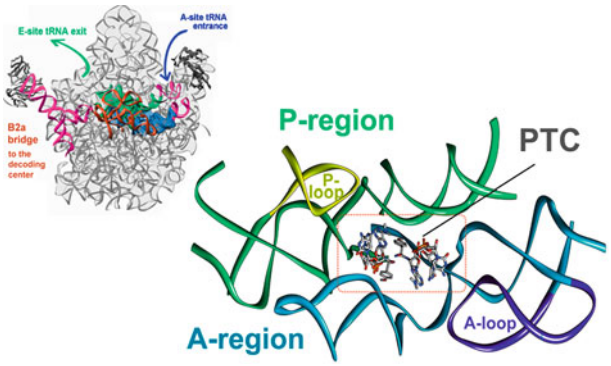

Fig. 4 The symmetrical region within the ribosome. Left: The symmetrical region within the ribosome and its details. The A-region is shown in blue, the P-region in green, and the non-symmetrical extensions are depicted in magenta. The bridge to the small subunit is shown in light brown. Right: Zoom into the symmetrical region, highlighting the basic structure that can form the active-site pocket and the loops that accommodate the C74 of the 3' ends of the A- and P-site tRNAs.

of peptide bonds by pure ribosomal RNA has not yet been demonstrated (Anderson et al., 2007).

The PTC is situated within a highly conserved universal symmetrical region that is embedded in the otherwise asymmetric ribosome structure (Figure 4). This region provides the machinery required for peptide bond formation, for the translocation of the A-site tRNA 3' end, for the detachment of the free substrate after peptide bond formation, and for the entry of the growing chain into the ribosome tunnel. This region is composed of 180 nucleotides, the fold, but not the sequence, of which is related by an internal pseudo two-fold symmetry. This region contains the two conserved nucleotides, G2552 and G2553, which form symmetrical Watson-Crick G-C base-pairs with the universally conserved CCA termini of the P and A-site tRNAs, respectively (Samaha et al., 1995; Kim and Green, 1999), and has been identified in all known ribosome structures, regardless of the source or functional state of the ribosomes (Bashan et al., 2003a; Zarivach et al., 2004; Agmon et al., 2005; Baram and Yonath, 2005). More specifically, the same sub-structure was identified in the cores of ribosomes from mesophilic, thermophilic, radiophilic and halophilic bacteria and archaea, regardless of their functional state or the ligands bound to them (Agmon et al., 2005). It is conceivable that the central location of the symmetrical region allows it to serve as the central signaling feature between all the functional regions involved in protein biosynthesis that are located remote from one another (up to 200 Å away), but must communicate during elongation (Uemura et al., 2007).

The PTC is built as an arched void located at the bottom of a V-shaped cavity that hosts the helical portion of the acceptor stems and the 3' ends (Figure 2) of both A- and P-site tRNAs (Figure 5). In the crystal structure of the large ribosomal subunit from *Deinococcus radiodurans* (D50S) in complex with a substrate analog that mimics the acceptor stem and the 3' end of the A-site tRNA (called acceptor stem mimic, ASM), the acceptor stem interacts extensively with the walls of the cavity (Bashan et al., 2003b), forming an elaborate network of interactions (Figure 5). These interactions dictate a specific orientation that facilitates the processivity of peptide bond formation. Thus, although the PTC has some tolerance in the positioning of "fragment reaction substrates" (Hansen et al., 2002), the interactions of the tRNA acceptor stem seem to be crucial for accurate substrate positioning in the PTC in a configuration allowing for peptide bond formation (Yonath, 2003). This structural observation supports the finding that the tRNA core region contributes to interactions with the ribosome (Pan et al., 2006). The linkage between the elaborate architecture of the symmetrical region and the position of the A-site tRNA suggests that the translocation of the tRNA 3' end within the PTC is related to the overall tRNA/mRNA translocation, assisted by EF-G, which is performed by a combination of two synchronized motions: a side-

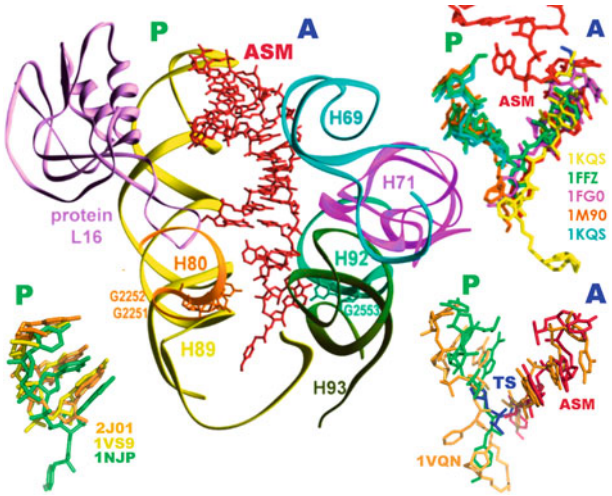

Fig. 5 Various substrates bound at the PTC. The central image shows the PTC and the cavity leading to it. The position of a mimic of A-site tRNA acceptor stem and 3' end (ASM, red) is shown. The components of the base pairs between the PTC upper rim (one at the A site and two in the P site) are highlighted. The RNA helices and the nucleotides located at the walls of the cavity are identified using *E. coli* numbering. Bottom left: Superposition of the 3' ends of P-site tRNAs: two experimentally determined (yellow and orange) and one derived (by rotation) moiety, in green. PDB entries are indicated by numbers. Top right: Positions and orientations of ASM and of various "minimal fragments" (puromycin derivatives) in the PTC; a dipeptide (yellow), produced by a minimal fragment that could not rotate into the P site because of its minimal size and its specific orientation, is shown in the A site. Bottom right: Superposition of ASM, the computed transition state (Gindulyte et al., 2006) (TS) and a chemically designed TS analog. Note that the extension of the chemical TS (Schmeing et al., 2005b), which is supposed to represent the nascent chain, is originating in the P site.

ways shift (the main component) and a rotatory motion of the A-site tRNA 3' end along a path confined by the PTC walls.

This rotatory motion appears to be navigated and guided by the ribosomal architecture, mainly the PTC rear wall that confines the rotatory path. Two flexible nucleotides, A2602 and U2585, seem to anchor and propel this motion. This means that the ribosomal architecture and its mobility provides all structural elements enabling ribosome function as an amino acid polymerase, including the formation of a symmetrical universal base pair between each of the tRNAs and the PTC (Bashan et al., 2003a; Agmon et al., 2005; Pan et al., 2006), alongside an additional base pair between the P-site tRNA and the PTC, a prerequisite for substrate-mediated acceleration (Weinger et al., 2004).

Importantly, all nucleotides involved in this rotatory motion have been classified as essential by a comprehensive genetic selection analysis (Sato et al., 2006). Furthermore, the rotatory motion positions the proximal 2'-hydroxyl of A76 of the P-site tRNA in the same position and orientation as found in crystals of the entire ribosome with mRNA and tRNAs (Korostelev et al., 2006a; Selmer et al., 2006) (Figure 5) and allows for chemical catalysis of peptide bond formation by A76 of the P-site tRNA (Weinger et al., 2004).

Simulation studies of the rotatory motion indicated that during this motion the rotating moiety interacts with ribosomal components confining the rotatory path, along the "PTC rear wall" (Agmon et al., 2005; Agmon et al., 2006). Consistently, quantum-mechanical calculations, based on D50S structural data, indicated that the transition state (TS) of peptide bond formation is formed during the rotatory motion and is stabilized by hydrogen bonds with rRNA nucleotides (Gindulyte et al., 2006). Importantly, the TS location suggested by quantum-mechanics is close to the location of a designed TS analog in the crystal structure of its complex with H50S (Schmeing et al., 2005) (Figure 5).

In short, the structure of D50S in complex with a substrate analog mimicking the part of the A-site tRNA that interacts with the large subunit advanced the comprehension of peptide bond formation by showing that ribosomes position their substrates in stereochemical configurations suitable for peptide bond formation (Bashan et al., 2003a; Agmon et al., 2005). Furthermore, the ribosomal architecture that facilitates positional catalysis of peptide bond formation, promotes substrate-mediated chemical acceleration, in accord with the requirement of full-length tRNAs for rapid and smooth peptide bond formation observed by various methods, including the usage of chemical, genetic (Polacek et al., 2001; Weinger et al., 2004; Youngman et al., 2004; Beringer et al., 2005; Polacek and Mankin, 2005; Brunelle et al., 2006; Sato et al., 2006), computational (Sharma et al., 2005; Gindulyte et al., 2006; Trobro and Aqvist, 2006) and kinetic studies (Beringer et al., 2005; Wohlgemuth et al., 2006; Beringer and Rodnina, 2007; Rodnina et al., 2007).

4. Structural disorder with functional meaning

The significance of the interactions of the acceptor stem with the cavity leading to the PTC was indicated by biochemical studies and clearly demonstrated crystallographically. Thus shedding light on the differences between the binding modes of full-size tRNA to 70S

ribosomes (or acceptor stem mimics to 50S subunits) and the binding modes of the various minimal substrates used for the fragment reaction. In functional experiments, the ribosome activity is determined by the reaction between substrate analogs capable of producing single peptide bonds. These "fragment reaction substrates" (Figure 5) are basically derivatives of puromycin, an A-site analog which acts as an inhibitor of the ribosomal polymerase activity. In many biochemical and structural studies, puromycin derivatives were used because they are good substrate analogs for a single peptide bond formation and because of the relative ease to detect in vitro single peptide bonds formed by them. However, caution is required when treating them as suitable to mimic the natural ribosome polymerase function. Interestingly, despite being small and consequently presumed to diffuse swiftly into its binding site within the ribosome, the rate of puromycin reaction with fMetPhe-tRNA as P-site substrate in 50S is comparable with rates of peptide bond formation with full-size tRNA (Wohlgemuth et al., 2008). It appears, therefore, that conformational rearrangements that were found to be required for productive positioning (Selmer et al., 2006) also play a role in determining the reaction rate. This idea is consistent with the biochemical finding that the peptidyl transfer reaction may be modulated by conformational changes at the active site (Youngman et al., 2004; Beringer et al., 2005; Schmeing et al., 2005; Brunelle et al., 2006; Beringer and Rodnina, 2007).

In the crystal structure of H50S with reactive fragment reaction substrates (Schmeing et al., 2002), the dipeptide resides in the A site (Figure 5) in an orientation hardly suitable for entrance into the tunnel. This complex was named "pre-translocational intermediate", meaning that in each elongation step the nascent protein has to translocate from the A to the P site. As the A to P site translocation within the PTC is performed by a 180 deg rotation, the translocation of the suggested "pre-translocational intermediate" requires that in each elongation step (15–20 times a second) such rotation is performed by the 3' end of A-site tRNA. If the entire growing chain is attached to its 3' end, it would have to rotate with it. Such motion would require a lot of space, which is probably not available in the dense PTC environment. Similarly, the energetic requirements of such a complicated operation should be very high. It appears, therefore that the dipeptide was trapped in the A site since the 3' end of the A-site tRNA did not undergo the rotatory motion because it, like all minimal substrate analogs, is too short and hence lacks moieties that facilitate the rotatory motion. Notably, the substrate was detected near the P site in the crystal structure of H50S with a substrate designed to mimic the transition state (Schmeing et al., 2005). As mentioned above, this finding is in accord with the results of the quantum mechanical computations that placed the transition state of the peptide bond in the PTC, close to the P site (Gindulyte et al., 2006). This result and the correlation between the rotatory motion and amino acid polymerization rationalize the detection of the dipeptide at the A site (Schmeing et al., 2002).

Hence, it appears that for the ribosome's polymerase activity the A-site substrate needs to be a full-length tRNA with its 3' end accurately positioned in the active site of the ribosome. This conclusion is supported by the study of a crystal structure of H50S in complex with a tRNA "mini-helix" (similar to the ASM described above) which led to the suggestion that specific rRNA nucleotides catalyze peptide bond formation by the general acid/base reverse mechanism (Ban et al., 2000), a proposition that was challenged by a number of biochemical and mutational studies, e. g. (Polacek et al., 2001).

Notably, in this structure, only the tip of the 3'-end is resolved, whereas the entire acceptor stem is disordered, presumably because its interactions with the partially disordered cavity leading to the PTC could not be formed (Nissen et al., 2000). Importantly, the H50S crystals used for this study were obtained under far from optimal functional conditions, namely rather low KCl concentration, while it was found that a very high KCl concentration is essential for the function of the ribosomes from the halophile *H. marismortui* (Shevack et al., 1985; Gluehmann et al., 2001).

The observed disorder in otherwise very well ordered crystals of H50S suggest that ribosomes kept under far from the conditions allowing for their efficient activity, can form peptide bonds but may not be capable of elongating nascent chains. This finding seems to point to a natural strategy for avoiding or minimizing the formation of proteins under stressful or far from physiological conditions. Specifically, the disorder of almost all of the functional regions of H50S may reflect a natural response of the halophilic ribosomes to a salt deficient environment, potentially indicating a natural mechanism for conserving cellular resources under stressful circumstances. In support of this suggestion, structural comparisons showed that the H50S active site contains key PTC components in orientations that differ significantly from those observed in empty D50S

(Harms et al., 2001) as well as in functional complexes of T70S ribosomes (Selmer et al., 2006).The main conclusion from the analyses of all of these structures is that single peptide bond formation can be performed even when the initial substrate binding is not accurate. However, for elongating the nascent proteins, accurate positioning of the A-site tRNA 3' end is mandatory. It appears, therefore, that the choice of substrate analogs for the various studies as well as the discrepancy between the definitions of ribosomal activity (namely the mere ability to form single peptide bonds versus the requirement for elongating nascent proteins) are the main reason for different structures, and potentially for their interpretation. It is clear that accurate substrate positioning within the ribosome frame, accompanied by the P-site tRNA interactions with 23S rRNA that allow for substrate catalysis (Weinger et al., 2004), plays the key role in ribosome catalytic functions, a notion that is currently widely accepted [e. g. (Beringer et al., 2005; Beringer and Rodnina, 2007; Simonovic and Steitz, 2008; Bashan and Yonath, 2008b)].

5. On the ribosomal tunnel and initial nascent protein folding

It was widely assumed that nascent proteins advance on the surface of the ribosome until their maturation. Even after biochemical experiments indicated that nascent chains are masked (hence protected) by the ribosome (Malkin and Rich, 1967; Sabatini and Blobel, 1970) and a tunnel was visualized in EM reconstructions from two-dimensional sheets at 60 and 25 Å resolution (Milligan and Unwin, 1986; Yonath et al., 1987), the existence of a tunnel was not generally accepted (Moore, 1988). Furthermore, it was assumed that nascent proteins are not degraded during protein synthesis because all of them adopt the conformation of an alpha helix (Ryabova et al., 1988). Doubts regarding the existence of the ribosomal tunnel were removed when it was visualized by cryo electron microscopy (Frank et al., 1995; Stark et al., 1995). Remarkably, the tunnel is of variable width and shape (Figure 3), suggesting its possible involvement in the fate of the nascent chains in accord with previous observations [e. g. (Crowley et al., 1993; Walter and Johnson, 1994)]. Furthermore, results of biochemical, microscopic, and computational experiments verified the existence of the tunnel and in several cases indicated that it may participate actively in nascent chain progression and its initial compaction, as well as in translation arrest and cellular signaling (Gabashvili et al., 2001; Gong and Yanofsky, 2002; Nakatogawa and Ito, 2002; Berisio et al., 2003; Gilbert et al., 2004; Johnson and Jensen, 2004; Woolhead et al., 2004; Amit et al., 2005; Ziv et al., 2005; Berisio et al., 2006; Cruz-Vera et al., 2006; Mankin, 2006; Mitra et al., 2006; Tenson and Mankin, 2006; Voss et al., 2006; Woolhead et al., 2006; Deane et al., 2007; Schaffitzel and Ban, 2007; Bornemann et al., 2008; Petrone et al., 2008; Starosta et al., 2010; Nakatogawa and Ito, 2004; Chiba et al., 2011).

While emerging from the ribosome, nascent chains may interact with chaperones that assist their folding and/or prevent their aggregation and misfolding. In bacteria the first chaperone that encounters the nascent proteins, called trigger factor, forms a shelter composed of hydrophobic and hydrophilic regions that provide an environment that can compete with the aggregation tendency of the still unfolded chains (Baram et al., 2005; Schluenzen et al., 2005; Kaiser et al., 2006). Interestingly, free trigger factor seems also to rescue proteins from misfolding and to accelerate protein folding (Martinez-Hackert and Hendrickson, 2009).

6. Antibiotics targeting the ribosome: strategies, expectations and problems

Because of the major significance of the ribosomes for cell viability many antibiotics target them. An immense amount of biochemical studies performed over four decades, alongside medical research and recent crystallographic analysis, showed that despite the high conservation of the ribosomal active sites, subtle differences facilitate their clinical relevance (Wilson, 2004; Yonath and Bashan, 2004; Polacek and Mankin, 2005; Yonath, 2005; Tenson and Mankin, 2006; Bottger, 2007; Sohmen et al., 2009). As so far there are no crystals of ribosomes from pathogenic organisms, structural information is currently obtained only from the crystallizable bacterial ribosomes that have been shown to be relevant as pathogen models, namely *E. coli, D. radiodurans,* and *T. thermophilus*. Antibiotic action on ribosomes from these bacteria, in conjunction with data obtained from the ribosomes of other organisms such as *Mycobacterium smegmatis* (a reasonable mimic of *Mycobacterium tuberculosis*), were found to be useful for determining antibiotic modes of action directly (described below) or indirectly (Pfister et al., 2005; Tu et al., 2005; Bommakanti et al., 2008; Hobbie et al., 2008).

The crystallographic analyses have shown that antibiotics targeting ribosomes exploit diverse strategies with common denominators. All antibioitcs target ribosomes at distinct locations within functionally relevant sites, mostly composed solely of rRNA. Each exerts its inhibitory action by competing with a crucial step in the biosynthetic cycle, including substrate binding, ribosomal dynamics, progression of the mRNA chain and decoding. Examples include hindering tRNA substrate accommodations at the PTC, stabilizing the tRNA in the A site in the pre-translocation state, preventing interactions of the ribosomal recycling factor and blocking the protein exit tunnel.

The identification of the various modes of action of antibiotics targeting ribosomes and an analysis of the ribosomal components comprising the binding pockets confirmed that the imperative distinction between ribosomes from eubacterial pathogens and mammalian cells hinges on subtle structural differences within the antibiotic binding pockets (Yonath and Bashan, 2004; Yonath, 2005; Pyetan et al., 2007; Auerbach et al., 2009; Auerbach et al., 2010). Apparently, fine tuning of the binding pocket can alter the binding parameters. These subtle sequence and/or conformational variations enable drug selectivity, thus facilitating clinical usage. Furthermore, the available structures illuminate features that are distinct between ribosomes from bacteria and non-pathogenic archaea that may be of crucial clinical importance.

Noteworthy are the results of comparisons between the crystal structures of different ribosomal particles complexed with the same antibiotics. Although leading to effective binding, disparities observed between the binding modes to pathogen models, namely *D. radiodurans* and *T. thermophilus*, may point to species specificity. Furthermore, comparison of the modes of antibiotic binding to ribosomal particles from the pathogen models (*D. radiodurans* and *T. thermophilus*) with modes observed in the archaeon *H. marismortui* (which shares properties with eukaryotes) indicated some variability in the binding modes, and in specific cases showed that binding is not synonymous with inhibitory activity. These comparisons highlighted the distinction between mere binding and binding leading to inhibitory activity. Specifically, for the macrolide family, these studies indicated that the identity of a single nucleotide can determine the strength of antibiotic binding, whereas proximal stereochemistry governs the antibiotic orientation within the binding pocket (Yonath and Bashan, 2004; Yonath, 2005) and consequently its therapeutic effectiveness. This is in accord with recent mutagenesis studies showing that mutation from guanine to adenine in 25S rRNA at the position equivalent to *E. coli* A2058 does not confer erythromycin sensitivity in *Saccharomyces cerevis*ae (Bommakanti et al., 2008). Thus, it was clearly demonstrated that the mere binding of an antibiotic is not sufficient for therapeutic effectiveness and that minute variations in the chemical moieties of the antibiotics can lead to significantly different binding modes. An appropriate example is the extreme difference between the modes of function of erythromycin, which competes with lankacidin binding, and lankamycin, which acts synergistically with lankacidin (Figure 6) (Auerbach et al., 2010; Belousoff et al., 2011).

In addition to rationalizing genetic, biochemical, and medical observations, the available structures have revealed unexpected inhibitory modes. Examples are the stabilization of the pre-translocation state (Stanley et al., 2010), as well as exploitation of the inherent ribosome flexibility for antibiotic synergism (Harms et al., 2004; Yonath, 2005; Auerbach et al., 2010) and for triggering an induced-fit mechanism by remote interactions that reshape the antibiotic binding pocket (Davidovich et al., 2007). Among the ribosomal antibiotics, the pleuromutilins are of special interest since they bind to the almost fully conserved PTC, yet they discriminate between bacterial and mammalian ribosomes. To circumvent the high conservation of the PTC, the pleuromutilins exploit the inherent functional mobility of the PTC and stabilize a conformational rearrangement that involves a network of remote interactions between flexible PTC nucleotides and less

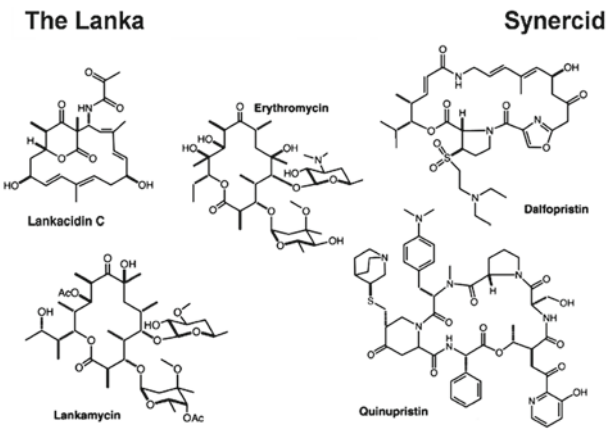

Fig. 6 The chemical compositions of antibiotic pairs acting on the ribosomal PTC and the exit tunnel. Both the lankacidin-lankamycin and the Synercid pairs display synergism. However, erythromycin (middle), which resembles lankamycin, competes with lankacidin.

conserved nucleotides residing in the PTC-vicinity (the second and third shells around the PTC). These interactions reshape the PTC contour and trigger its closure on the bound drug (Davidovich et al., 2007). The uniqueness of this pleuromutilin binding mode led to new insights as it indicated the existence of an allosteric network around the ribosomal active site. Indeed, the value of these findings is far beyond their perspective on clinical usage, as they highlight basic issues, such as the possibility of remote reshaping of binding pockets and the ability of ribosome inhibitors to benefit from the inherent flexibility of the ribosome.

Similar to the variability in binding modes, seemingly identical mechanisms of drug resistance can indeed be different, as they are dominated, directly or via cellular effects, by the antibiotics' chemical properties (Davidovich et al., 2007; Davidovich et al., 2008). The observed variability in antibiotic binding and inhibitory modes justifies expectations for structurally based improvement of the properties of existing compounds as well as for the development of novel drug classes. Detailed accounts can be found in several reviews (Auerbach et al., 2004; Yonath and Bashan, 2004; Poehlsgaard and Douthwaite, 2005; Yonath, 2005; Bottger, 2006; Tenson and Mankin, 2006; Bottger, 2007).

In short, over two dozen three-dimensional structures of ribosome complexes with antibiotics have revealed the principles allowing for clinical use, have provided unparalleled insight into the mode of antibiotic function, have illuminated mechanisms for acquiring resistance and have shown the basis for discrimination between pathogens and host cells. The elucidation of common principles of the mode of action of antibiotics targeting the ribosome combined with variability in binding modes led to the uncovering of diverse mechanisms for acquiring antibiotic resistance.

7. The ribosomal core is the optimized vestige of an ancient entity

A high level of sequence conservation in the symmetrical region has been maintained throughout ribosome evolution, even in mitochondrial ribosomes in which half the ribosomal RNA has been replaced by proteins (Mears et al., 2002; Thompson and Dahlberg, 2004; Agmon et al., 2006; Davidovich et al., 2009). This conservation and the observation that the symmetrical region provide all structural elements required for performing polypeptide elongation led us to suggest that the modern ribosome evolved by gene fusion or gene duplication (Figure 7). We refer to this ancestral entity as the proto-ribosome (Agmon et al., 2005; Davidovich et al., 2009; Belousoff et al., 2010a; Belousoff et al., 2010b).

In particular, the preservation of the three-dimensional structure of the two halves of the ribosomal frame, independent of the sequence, emphasizes the superiority of functional requirements over sequence conservation and demonstrates the rigorous requirements of accurate substrate positioning for peptide bond formation. As mentioned above, this, as well as the universality of the symmetrical region, led to the assumption that the ancient ribosome was composed of a pocket confined by two RNA chains that formed a dimer, and that this pocket is still embedded in the heart of the modern ribosome (Figures 4, 7). In fact, as mentioned above, suggestions that proteins are made by an RNA machine have been made already in the sixties (Crick, 1968), and extensive research over the past three decades (summarized in a recent book (Yarus, 2010)) has supported the idea that nucleic acids are capable of independent replication, selection, and self splicing [e. g. (Been and Cech, 1986; Abelson, 1990; Ellington and Szostak, 1990; Tuerk and Gold, 1990; Pino et al., 2008; Costanzo et al., 2009; Lincoln and Joyce, 2009)].

In accord with these findings we have proposed (Agmon et al., 2006; Davidovich et al., 2009; Belousoff et al., 2010a; Belousoff et al., 2010b; Turk et al., 2010) that the ancient machinery that could form peptide bonds was made exclusively from RNA molecules, utilizing substituents available in the primordial soup, namely RNA chains that could acquire conformations sufficiently stable to survive evolutionary stress.

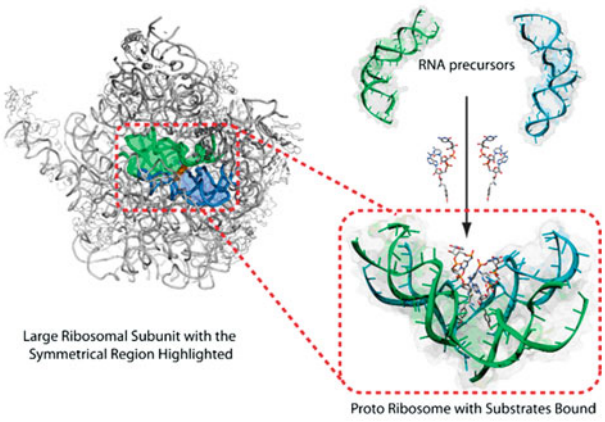

Fig. 7 The suggested proto-ribosome. Regions hosting A- and P-site tRNAs are shown in blue and green, respectively. The A-site tRNA mimic (Bashan et al., 2003) is shown in blue, and the derived P-site tRNA (by the rotatory motion) is shown in green.

These ancient RNA chains could fold spontaneously and then dimerize. The products of the dimerization yielded three-dimensional structures with a symmetrical pocket that could accommodate small substrates (e. g. amino acids conjugated with mono or oligo RNA nucleotides) in a stereochemistry suitable for spontaneous formation of various chemical bonds, including the peptide bond. These dimeric RNA complexes could have become the ancestors of the symmetrical region in the contemporary ribosome. The most appropriate pockets for promoting peptide bond formation survived.

The surviving ancient pockets became the templates for the ancient ribosomes. In a later stage, these initial RNA genes underwent optimization to produce more defined, relatively stable pockets, and when the correlation between the amino acid and the growing peptidyl sites was established, each of the two halves was further optimized for its task so that their sequences evolved differently. The entire ribosome could have evolved gradually around this symmetrical region until it acquired its final shape (Bokov and Steinberg, 2009).

The substrates of the ancient ribosomes, which were initially spontaneously produced amino acids conjugated with single or short oligo-nucleotides (Illangasekare et al., 1995; Turk et al., 2010), could have evolved in parallel to allow accurate binding, as occurs for aminoacylated CCA 3'-end. Later on, these could have been converted into longer compounds with a contour that can complement the inner surface of the reaction pocket. For increasing specificity, these short RNA segments could have been extended to larger entities by their fusion with stable RNA features, to form the ancient tRNA, presumably capable of storing, selecting and transferring instructions for producing useful proteins. The structural entity for decoding could have been combined with the structural machinery able to form a peptide bond in a single entity. Adding a feature similar to the modern anticodon loop allowed some genetic control, and could have led to the modern protein-nucleic acids world.

8. Conclusion

The currently available high-resolution structures of ribosomes and their subunits proved that the ribosome is a ribozyme. All functions of the ribosome, including decoding, peptide bond formation, protein elongation and tRNA release, are performed by ribosomal RNA while being assisted by ribosomal proteins.

A key requirement for highly efficient processivity of the ribosome's main catalytic activities hinges on accurate positioning of the ribosomal substrate, which hinges on the maintenance of the functional conformations of all ribosomal regions involved in ribosomal function, despite their high flexibility. Hence, disorder of these regions has functional meaning, and may be the result of a natural strategy to minimize cell function under hostile conditions.

The ribosomal active site, namely where the peptide bonds are being formed and where the nascent chain is elongated, is situated within a universal symmetrical region that is embedded in the otherwise asymmetric ribosome structure. This symmetrical region is highly conserved and provides the machinery required for peptide bond formation as well as for the ribosome polymerase activity. Therefore, it may be the remnant of the proto-ribosome, which seems to be a dimeric prebiotic machine that initially catalyzed prebiotic reactions, including the formation of chemical bonds, and then produced non-coded oligopeptides.

Structures of complexes of ribosomes with antibiotics revealed principles allowing for the clinical use of antibiotics, identified resistance mechanisms, and pointed at the structural basis for discriminating pathogenic bacteria from hosts. Thus, structural analyses provided valuable information for the improvement of antibiotics and for the design of novel compounds that can serve as antibiotics.

9. Future prospects

Ribosome research has undergone astonishing progress in recent years. The high-resolution structures have shed light on many of the functional properties of the translation machinery and revealed how the ribosome's striking architecture is ingeniously designed as the framework for its unique capabilities: precise decoding, substrate mediated peptide-bond formation and efficient polymerase activity. By analyzing these structures it appears that the ribosomal tasks are performed by the ribosomal RNA and may be supported by the ribosomal proteins.

Among the new findings that emerged from the structures are the intricate mode of decoding, the mobility of most of the ribosomal functional features, the symmetrical region at the core of the ribosome, the dynamic properties of the ribosomal tunnel, the interactions of the ribosome with the progressing nascent

chains, the signaling between the ribosome and cellular components, and the shelter formed by the first chaperone that encounters the nascent chains (trigger factor) for preventing nascent chain aggregation and misfolding. Novel insights from these new findings include the suggestion that the translocation of the tRNA involves at least two concerted motions: sideways shift (which may be performed in a hybrid mode) and a ribosome-navigated rotation. The linkage between these findings and crystal structures of ribosomes with over two dozen antibiotics targeting the ribosome, illuminated various modes of binding and action of these antibiotics. They also deciphered mechanisms leading to resistance and identified the principles allowing for the discrimination between pathogens and eukaryotes despite high ribosome conservation. Further studies enlightened the basis for antibiotic synergism (Figure 6), indicated correlations between antibiotic susceptibility and fitness cost, and revealed a novel induced-fit mechanism exploiting inherent ribosomal flexibility for reshaping the antibiotic binding pocket by remote interactions. Thus, the high-resolution structures of the complexes of the ribosomes with the antibiotics bound to them address key issues associated with the structural basis for antibiotic resistance, synergism, and selectivity and provide unique structural tools for improving antibiotic action.

The availability of the high-resolution structures has stimulated an unpredictable expansion in ribosome research, which in turn has resulted in new insights into the translation process. An appropriate example is the study on real-time tRNA transit on single translating ribosomes at codon resolution (Uemura et al., 2010). However, despite the extensive research and the immense progress, several key issues are still unresolved, some of which are described above. Thus, it is clear that the future of ribosome research and its applications hold more scientific excitement.

Acknowledgements

Thanks are due to all members of the ribosome groups at the Weizmann Institute and at the Unit for Ribosome Research of the Max Planck Society at DESY/Hamburg for their experimental efforts and illuminating discussion. Support was provided by the US National Inst. of Health (GM34 360), the German Ministry for Science and Technology (BMBF 05–641EA), GIF 853–2004, Human Frontier Science Program (HFSP) RGP0076/2003 and the Kimmelman Center for Macromolecular Assemblies. AY holds the Martin and Helen Kimmel Professorial Chair. X-ray diffraction data were collected the EMBL and MPG beam lines at DESY; F1/CHESS, Cornell University, SSRL/Stanford University, ESRF/EMBL, Grenoble, BL26/PF/KEK, Japan, and 19ID&23ID/APS/Argonne National Laboratory.

References

Abelson J (1990) Directed evolution of nucleic acids by independent replication and selection. Science 249: 488–489

Agmon I, Bashan A, Yonath A (2006) On Ribosome Conservation and Evolution. Isr J Ecol Evol 52: 359–379

Agmon I, Bashan A, Zarivach R, Yonath A (2005) Symmetry at the active site of the ribosome: structural and functional implications. Biol Chem 386: 833–844

Amit M, Berisio R, Baram D, Harms J, Bashan A, Yonath A (2005) A crevice adjoining the ribosome tunnel: hints for cotranslational folding. FEBS Lett 579: 3207–3213

Anderson RM, Kwon M, Strobel SA (2007) Toward ribosomal RNA catalytic activity in the absence of protein. J Mol Evol 64: 472–483

Auerbach-Nevo T, Zarivach R, Peretz M, Yonath A (2005) Reproducible growth of well diffracting ribosomal crystals. Acta Crystallogr D Biol Crystallogr 61: 713–719

Auerbach T, Bashan A, Yonath A (2004) Ribosomal antibiotics: structural basis for resistance, synergism and selectivity. Trends Biotechnol 22: 570–576

Auerbach T, Mermershtain I, Bashan A, Davidovich C, Rosenberg H, Sherman DH, Yonath A (2009) Structural basis for the antibacterial activity of the 12-membered-ring mono-sugar macrolide methymycin. Biotechnolog 84: 24–35

Auerbach T, Mermershtain I, Davidovich C, Bashan A, Belousoff M, Wekselman I, Zimmerman E, Xiong L, Klepacki D, Arakawa K, Kinashi H, Mankin AS, Yonath A (2010) The structure of ribosome-lankacidin complex reveals ribosomal sites for synergistic antibiotics. Proc Natl Acad Sci USA 107: 1983–1988

Ban N, Nissen P, Hansen J, Moore PB, Steitz TA (2000) The complete atomic structure of the large ribosomal subunit at 2.4 A resolution. Science 289: 905–920

Baram D, Pyetan E, Sittner A, Auerbach-Nevo T, Bashan A, Yonath A (2005) Structure of trigger factor binding domain in biologically homologous complex with eubacterial ribosome reveals its chaperone action. Proc Natl Acad Sci USA 102: 12 017–12 022

Baram D, Yonath A (2005) From peptide-bond formation to cotranslational folding: dynamic, regulatory and evolutionary aspects. FEBS Lett 579: 948–954

Bashan A, Agmon I, Zarivach R, Schluenzen F, Harms J, Berisio R, Bartels H, Franceschi F, Auerbach T, Hansen HA, Kossoy E, Kessler M, Yonath A (2003a) Structural basis of the ribosomal machinery for peptide bond formation, translocation, and nascent chain progression. Mol Cell 11: 91–102

Bashan A, Agmon I, Zarivach R, Schluenzen F, Harms J, Berisio R, Bartels H, Franceschi F, Auerbach T, Hansen HAS, Kossoy E, Kessler M, Yonath A (2003b) Structural basis of the ribosomal machinery for peptide bond formation, translocation, and nascent chain progression. Mol Cell 11: 91–102

Bashan A, Yonath A (2008a) The linkage between ribosomal crystallography, metal ions, heteropolytungstates and functional flexibility. J Mol Struct 890 289–294

Bashan A, Yonath A (2008b) Correlating ribosome function with high-resolution structures. Trends Microbiol 16: 326–335

Been MD, Cech TR (1986) One binding site determines sequence specificity of Tetrahymena pre-rRNA self-splicing, trans-splicing, and RNA enzyme activity. Cell 47: 207–216

Belousoff M, Davidovich C, Bashan A, Yonath A (2010a) in the press. Orig Life Evol Biosph

Belousoff MJ, Shapira,T, Bashan A, Zimmerman E, Rozenberg H, Arakawa K, Kinashi H, Yonath A (2011) Crystal structure of the synergistic antibiotic pair lankamycin and lankacidin in complex with the large ribosomal subunit. Proc Nat Acad USA; e-pub Feb 2011

Belousoff MJ, Davidovich C, Zimmerman E, Caspi Y, Wekselman I, Rozenszajn L, Shapira T, Sade-Falk O, Taha L, Bashan A, Weiss MS, Yonath A (2010b) Ancient machinery embedded in the contemporary ribosome. Biochem Soc Trans 38: 422–427

Beringer M, Bruell C, Xiong L, Pfister P, Bieling P, Katunin VI, Mankin AS, Bottger EC, Rodnina MV (2005) Essential mechanisms in the catalysis of peptide bond formation on the ribosome. J Biol Chem 280: 36 065–36 072

Beringer M, Rodnina MV (2007) The ribosomal peptidyl transferase. Mol Cell 26: 311–321

Berisio R, Corti N, Pfister P, Yonath A, Bottger EC (2006) 23S rRNA 2058A->G Alteration Mediates Ketolide Resistance in Combination with Deletion in L22. Antimicrob Agents Chemother 50: 3816–3823

Berisio R, Schluenzen F, Harms J, Bashan A, Auerbach T, Baram D, Yonath A (2003) Structural insight into the role of the ribosomal tunnel in cellular regulation. Nat Struct Biol 10: 366–370

Blaha G, Stanley RE, Steitz TA (2009) Formation of the first peptide bond: the structure of EF-P bound to the 70S ribosome. Science 325: 966–970

Bokov K, Steinberg SV (2009) A hierarchical model for evolution of 23S ribosomal RNA. Nature 457: 977–980

Bommakanti AS, Lindahl L, Zengel JM (2008) Mutation from guanine to adenine in 25S rRNA at the position equivalent to *E. coli* A2058 does not confer erythromycin sensitivity in Sacchromyces cerevisae. RNA 14: 460–464

Bornemann T, Jockel J, Rodnina MV, Wintermeyer W (2008) Signal sequence-independent membrane targeting of ribosomes containing short nascent peptides within the exit tunnel. Nat Struct Mol Biol 15: 494–499

Borovinskaya MA, Pai RD, Zhang W, Schuwirth BS, Holton JM, Hirokawa G, Kaji H, Kaji A, Cate JH (2007) Structural basis for aminoglycoside inhibition of bacterial ribosome recycling. Nat Struct Mol Biol 14: 727–732

Bottger EC (2006) The ribosome as a drug target. Trends Biotechnol 24: 145–147

Bottger EC (2007) Antimicrobial agents targeting the ribosome: the issue of selectivity and toxicity – lessons to be learned. Cell Mol Life Sci 64: 791–795

Brunelle JL, Youngman EM, Sharma D, Green R (2006) The interaction between C75 of tRNA and the A loop of the ribosome stimulates peptidyl transferase activity. RNA 12: 33–39

Carter AP, Clemons WM, Jr., Brodersen DE, Morgan-Warren RJ, Hartsch T, Wimberly BT, Ramakrishnan V (2001) Crystal structure of an initiation factor bound to the 30S ribosomal subunit. Science 291: 498–501

Chiba S, Kanamori T, Ueda T, Akiyama Y, Pogliano, K, Ito, K (2011) Recruitment of a species-specific arrest module to monitor different cellular processes. Proc Natl Acad Sci USA; e pub March 2011

Costanzo G, Pino S, Ciciriello F, Di Mauro E (2009) Generation of long RNA chains in water. J Biol Chem 284: 33 206–33 216

Crick FH (1968) The origin of the genetic code. J Mol Biol 38: 367–379

Crowley KS, Reinhart GD, Johnson AE (1993) The signal sequence moves through a ribosomal tunnel into a noncytoplasmic aqueous environment at the ER membrane early in translocation. Cell 73: 1101–1115

Cruz-Vera LR, Gong M, Yanofsky C (2006) Changes produced by bound tryptophan in the ribosome peptidyl transferase center in response to TnaC, a nascent leader peptide. Proc Natl Acad Sci USA 103: 3598–3603

Davidovich C, Bashan A, Auerbach-Nevo T, Yaggie RD, Gontarek RR, Yonath A (2007) Induced-fit tightens pleuromutilins binding to ribosomes and remote interactions enable their selectivity. Proc Natl Acad Sci USA 104: 4291–4296

Davidovich C, Bashan A, Yonath A (2008) Structural basis for cross-resistance to ribosomal PTC antibiotics. Proc Natl Acad Sci USA 105: 20 665–20 670

Davidovich C, Belousoff M, Bashan A, Yonath A (2009) The evolving ribosome: from non-coded peptide bond formation to sophisticated translation machinery. Res Microbiol 160: 487–492

Deane CM, Dong M, Huard FP, Lance BK, Wood GR (2007) Cotranslational protein folding–fact or fiction? Bioinformatics 23:i142–148

Demeshkina N, Jenner L, Yusupova G, Yusupov M (2010) Interactions of the ribosome with mRNA and tRNA. Curr Opin Struct Biol:12

Ellington AD, Szostak JW (1990) In vitro selection of RNA molecules that bind specific ligands. Nature 346: 818–822

Frank J, Zhu J, Penczek P, Li Y, Srivastava S, Verschoor A, Radermacher M, Grassucci R, Lata RK, Agrawal RK (1995) A model of protein synthesis based on cryo-electron microscopy of the *E. coli* ribosome. Nature 376: 441–444

Gabashvili IS, Gregory ST, Valle M, Grassucci R, Worbs M, Wahl MC, Dahlberg AE, Frank J (2001) The polypeptide tunnel system in the ribosome and its gating in erythromycin resistance mutants of L4 and L22. Mol Cell 8: 181–188

Garrett RA, Wittmann HG (1973) Structure and function of the ribosome. Endeavour 32: 8–14

Gilbert RJ, Fucini P, Connell S, Fuller SD, Nierhaus KH, Robinson CV, Dobson CM, Stuart DI (2004) Three-Dimensional Structures of Translating Ribosomes by Cryo-EM. Mol Cell 14: 57–66

Gindulyte A, Bashan A, Agmon I, Massa L, Yonath A, Karle J (2006) The transition state for formation of the peptide bond in the ribosome. Proc Natl Acad Sci USA 103: 13 327–13 332

Gluehmann M, Zarivach R, Bashan A, Harms J, Schluenzen F, Bartels H, Agmon I, Rosenblum G, Pioletti M, Auerbach T, Avila H, Hansen HA, Franceschi F, Yonath A (2001) Ribosomal crystallography: from poorly diffracting microcrystals to high-resolution structures. Methods 25: 292–302

Gong F, Yanofsky C (2002) Instruction of translating ribosome by nascent Peptide. Science 297: 1864–1867

Hansen HA, Volkmann N, Piefke J, Glotz C, Weinstein S, Makowski I, Meyer S, Wittmann HG, Yonath A (1990) Crystals of complexes mimicking protein biosynthesis are suitable for crystallographic studies. Biochim Biophys Acta 1050: 1–7

Hansen JL, Schmeing TM, Moore PB, Steitz TA (2002) Structural insights into peptide bond formation. Proc Natl Acad Sci USA 99: 11 670–11 675

Harms J, Schluenzen F, Fucini P, Bartels H, Yonath A (2004) Alterations at the peptidyl transferase centre of the ribosome induced by the synergistic action of the streptogramins dalfopristin and quinupristin. BMC Biol 2: 4;1–10

Harms J, Schluenzen F, Zarivach R, Bashan A, Gat S, Agmon I, Bartels H, Franceschi F, Yonath A (2001) High resolution structure of the large ribosomal subunit from a mesophilic eubacterium. Cell 107: 679–688

Hobbie SN, Bruell CM, Akshay S, Kalapala SK, Shcherbakov D, Bottger EC (2008) Mitochondrial deafness alleles confer misreading of the genetic code. Proc Natl Acad Sci USA 105: 3244–3249

Hope H, Frolow F, von Bohlen K, Makowski I, Kratky C, Halfon Y, Danz H, Webster P, Bartels KS, Wittmann HG, et al. (1989) Cryocrystallography of ribosomal particles. Acta Crystallogr B 45: 190–199

Illangasekare M, Sanchez G, Nickles T, Yarus M (1995) Aminoacyl-RNA synthesis catalyzed by an RNA. Science 267: 643–647

Jenner L, Ito K, Rees B, Yusupov M, Yusupova G (2007) Messenger RNA conformations in the ribosomal E site revealed by X-ray crystallography. EMBO Rep 8: 846–850

Jenner LB, Demeshkina N, Yusupova G, Yusupov M (2010) Structural aspects of messenger RNA reading frame maintenance by the ribosome. Nat Struct Mol Biol 17: 555–560

Johnson AE, Jensen RE (2004) Barreling through the membrane. Nat Struct Mol Biol 11: 113–114

Kaiser CM, Chang HC, Agashe VR, Lakshmipathy SK, Etchells SA, Hayer-Hartl M, Hartl FU, Barral JM (2006) Real-time observation of trigger factor function on translating ribosomes. Nature 444: 455–460

Kim DF, Green R (1999) Base-pairing between 23S rRNA and tRNA in the ribosomal A site. Mol Cell 4: 859–864

Korostelev A, Trakhanov S, Laurberg M, Noller HF (2006a) Crystal structure of a 70S ribosome-tRNA complex reveals functional interactions and rearrangements. Cell 126: 1065–1077

Korostelev A, Trakhanov S, Laurberg M, Noller HF (2006b) Crystal Structure of a 70S Ribosome-tRNA Complex Reveals Functional Interactions and Rearrangements. Cell 126: 1065–1077

Laurberg M, Asahara H, Korostelev A, Zhu J, Trakhanov S, Noller HF (2008) Structural basis for translation termination on the 70S ribosome. Nature 454: 852–857

Lincoln TA, Joyce GF (2009) Self-Sustained Replication of an RNA Enzyme. Science 323: 1229–1232

Malkin LI, Rich A (1967) Partial resistance of nascent polypeptide chains to proteolytic digestion due to ribosomal shielding. J Mol Biol 26: 329–346

Mankin A (2006) Antibiotic blocks mRNA path on the ribosome. Nat Struct Mol Biol 13: 858–860

Martinez-Hackert E, Hendrickson WA (2009) Promiscuous substrate recognition in folding and assembly activities of the trigger factor chaperone. Cell 138: 923–934

Mears JA, Cannone JJ, Stagg SM, Gutell RR, Agrawal RK, Harvey SC (2002) Modeling a minimal ribosome based on comparative sequence analysis. J Mol Biol 321: 215–234

Milligan RA, Unwin PN (1986) Location of exit channel for nascent protein in 80S ribosome. Nature 319: 693–695

Mitra K, Schaffitzel C, Fabiola F, Chapman MS, Ban N, Frank J (2006) Elongation arrest by SecM via a cascade of ribosomal RNA rearrangements. Mol Cell 22: 533–543

Moore PB (1988) The ribosome returns. Nature 331: 223–227

Nakatogawa H, Ito K (2004) Intraribosomal Regulation of Expression and Fate of Proteins ChemBioChem 5: 48-51

Nakatogawa H, Ito K (2002) The ribosomal exit tunnel functions as a discriminating gate. Cell 108: 629–636

Nissen P, Hansen J, Ban N, Moore PB, Steitz TA (2000) The structural basis of ribosome activity in peptide bond synthesis. Science 289: 920–930

Noller HF, Hoffarth V, Zimniak L (1992) Unusual resistance of peptidyl transferase to protein extraction procedures. Science 256: 1416–1419

Palade GE (1955) A small particulate component of the cytoplasm. J Biophys Biochem Cytol 1: 59–68

Pan D, Kirillov S, Zhang CM, Hou YM, Cooperman BS (2006) Rapid ribosomal translocation depends on the conserved 18–55 base pair in P-site transfer RNA. Nat Struct Mol Biol 13: 354–359

Petrone PM, Snow CD, Lucent D, Pande VS (2008) Side-chain recognition and gating in the ribosome exit tunnel. Proc Natl Acad Sci USA 105: 16 549–16 554

Pfister P, Corti N, Hobbie S, Bruell C, Zarivach R, Yonath A, Bottger EC (2005) 23S rRNA base pair 2057–2611 determines ketolide susceptibility and fitness cost of the macrolide resistance mutation 2058A → G. Proc Natl Acad Sci USA 102: 5180–5185

Pino S, Ciciriello F, Costanzo G, Di Mauro E (2008) Nonenzymatic RNA ligation in water. J Biol Chem 283: 36 494–36 503

Pioletti M, Schluenzen F, Harms J, Zarivach R, Gluehmann M, Avila H, Bashan A, Bartels H, Auerbach T, Jacobi C, Hartsch T, Yonath A, Franceschi F (2001) Crystal structures of complexes of the small ribosomal subunit with tetracycline, edeine and IF3. Embo J 20: 1829–1839

Poehlsgaard J, Douthwaite S (2005) The bacterial ribosome as a target for antibiotics. Nat Rev Microbiol 3: 870–881

Polacek N, Gaynor M, Yassin A, Mankin AS (2001) Ribosomal peptidyl transferase can withstand mutations at the putative catalytic nucleotide. Nature 411: 498–501

Polacek N, Mankin AS (2005) The ribosomal peptidyl transferase center: structure, function, evolution, inhibition. Crit Rev Biochem Mol Biol 40: 285–311

Pyetan E, Baram D, Auerbach-Nevo T, Yonath A (2007) Chemical parameters influencing fine-tuning in the binding of macrolide antibiotics to the ribosomal tunnel. Pure Appl Chem 79: 955–968

Ramakrishnan V (2008) What we have learned from ribosome structures. Biochem Soc Trans 36: 567–574

Rodnina MV, Beringer M, Wintermeyer W (2007) How ribosomes make peptide bonds. Trends Biochem Sci 32: 20–26

Ryabova LA, Selivanova OM, Baranov VI, Vasiliev VD, Spirin AS (1988) Does the channel for nascent peptide exist inside the ribosome? Immune electron microscopy study. FEBS Lett 226: 255–260

Sabatini DD, Blobel G (1970) Controlled proteolysis of nascent polypeptides in rat liver cell fractions. II. Location of the polypeptides in rough microsomes. J Cell Biol 45: 146–157

Samaha RR, Green R, Noller HF (1995) A base pair between tRNA and 23S rRNA in the peptidyl transferase centre of the ribosome. Nature 377: 309–314

Sato NS, Hirabayashi N, Agmon I, Yonath A, Suzuki T (2006) Comprehensive genetic selection revealed essential bases in the peptidyl-transferase center. Proc Natl Acad Sci USA 103: 15 386–15 391

Schaffitzel C, Ban N (2007) Generation of ribosome nascent chain complexes for structural and functional studies. J Struct Biol 158: 463–471

Schluenzen F, Tocilj A, Zarivach R, Harms J, Gluehmann M, Janell D, Bashan A, Bartels H, Agmon I, Franceschi F, Yonath A

(2000) Structure of functionally activated small ribosomal subunit at 3.3 angstroms resolution. Cell 102: 615–623

Schluenzen F, Wilson DN, Tian P, Harms JM, McInnes SJ, Hansen HA, Albrecht R, Buerger J, Wilbanks SM, Fucini P (2005) The Binding Mode of the Trigger Factor on the Ribosome: Implications for Protein Folding and SRP Interaction. Structure (Camb) 13: 1685–1694

Schmeing TM, Huang KS, Kitchen DE, Strobel SA, Steitz TA (2005) Structural Insights into the Roles of Water and the 2' Hydroxyl of the P Site tRNA in the Peptidyl Transferase Reaction. Mol Cell 20: 437–448

Schmeing TM, Seila AC, Hansen JL, Freeborn B, Soukup JK, Scaringe SA, Strobel SA, Moore PB, Steitz TA (2002) A pretranslocational intermediate in protein synthesis observed in crystals of enzymatically active 50S subunits. Nat Struct Biol 9: 225–230

Schmeing TM, Voorhees RM, Kelley AC, Gao YG, Murphy FVt, Weir JR, Ramakrishnan V (2009) The Crystal Structure of the Ribosome Bound to EF-Tu and Aminoacyl-tRNA. Science 326: 688–694

Schuwirth BS, Borovinskaya MA, Hau CW, Zhang W, Vila-Sanjurjo A, Holton JM, Cate JHD (2005) Structures of the Bacterial Ribosome at 3.5 A Resolution. Science 310: 827–834

Selmer M, Dunham CM, Murphy Iv FV, Weixlbaumer A, Petry S, Kelley AC, Weir JR, Ramakrishnan V (2006) Structure of the 70S Ribosome Complexed with mRNA and tRNA. Science 313: 1935–1942

Sharma PK, Xiang Y, Kato M, Warshel A (2005) What Are the Roles of Substrate-Assisted Catalysis and Proximity Effects in Peptide Bond Formation by the Ribosome? Biochemistry 44: 11 307–11 314

Shevack A, Gewitz HS, Hennemann B, Yonath A, Wittmann HG (1985) Characterization and crystallization of ribosomal particles from Halobacterium marismortui. FEBS Lett 184: 68–71

Simonetti A, Marzi S, Jenner L, Myasnikov A, Romby P, Yusupova G, Klaholz BP, Yusupov M (2009) A structural view of translation initiation in bacteria. Cell Mol Life Sci 66: 423–436

Simonetti A, Marzi S, Myasnikov AG, Fabbretti A, Yusupov M, Gualerzi CO, Klaholz BP (2008) Structure of the 30S translation initiation complex. Nature 455: 416–420

Simonovic M, Steitz TA (2008) Peptidyl-CCA deacylation on the ribosome promoted by induced fit and the O3'-hydroxyl group of A76 of the unacylated A-site tRNA. RNA 14: 2372–2378

Sohmen D, Harms JM, Schlunzen F, Wilson DN (2009) Enhanced SnapShot: Antibiotic inhibition of protein synthesis II. Cell 139: 212–212

Stanley RE, Blaha G, Grodzicki RL, Strickler MD, Steitz TA (2010) The structures of the anti-tuberculosis antibiotics viomycin and capreomycin bound to the 70S ribosome. Nat Struct Mol Biol 17: 289–293

Stark H, Mueller F, Orlova EV, Schatz M, Dube P, Erdemir T, Zemlin F, Brimacombe R, van Heel M (1995) The 70S *Escherichia coli* ribosome at 23 A resolution: fitting the ribosomal RNA. Structure 3: 815–821

Starosta AL, Karpenko VV, Shishkina AV, Mikolajka A, Sumbatyan NV, Schluenzen F, Korshunova GA, Bogdanov AA, Wilson DN (2010) Interplay between the ribosomal tunnel, nascent chain, and macrolides influences drug inhibition. Chem Biol 17: 504–514

Tenson T, Mankin A (2006) Antibiotics and the ribosome. Mol Microbiol 59: 1664–1677

Thompson J, Dahlberg AE (2004) Testing the conservation of the translational machinery over evolution in diverse environments: assaying Thermus thermophilus ribosomes and initiation factors in a coupled transcription-translation system from *Escherichia coli*. Nucleic Acids Res 32: 5954–5961

Thygesen J, Krumbholz S, Levin I, Zaytzevbashan A, Harms J, Bartels H, Schlunzen F, Hansen HAS, Bennett WS, Volkmann N, Agmon I, Eisenstein M, Dribin A, Maltz E, Sagi I, Morlang S, Fua M, Franceschi F, Weinstein S, Boddeker N, Sharon R, Anagnostopoulos K, Peretz M, Geva M, Berkovitchyellin Z, Yonath A (1996) Ribosomal crystallography – from crystal growth to initial phasing. J Cryst Growth 168: 308–323

Trakhanov SD, Yusupov MM, Agalarova SC, Garber MB, Ryazantseva SN, Tischenko SV, Shirokova VA (1987) Crystallization of 70 S ribosomes and 30 S ribosomal subunits from Thermus thermophilus. FEBS Lett 220: 319–322

Trobro S, Aqvist J (2006) Analysis of predictions for the catalytic mechanism of ribosomal peptidyl transfer. Biochemistry 45: 7049–7056

Tu D, Blaha G, Moore PB, Steitz TA (2005) Structures of MLSBK Antibiotics Bound to Mutated Large Ribosomal Subunits Provide a Structural Explanation for Resistance. Cell 121: 257–270

Tuerk C, Gold L (1990) Systematic evolution of ligands by exponential enrichment: RNA ligands to bacteriophage T4 DNA polymerase. Science 249: 505–510

Turk RM, Chumachenko NV, Yarus M (2010) Multiple translational products from a five-nucleotide ribozyme. Proc Natl Acad Sci USA 107: 4585–4589

Uemura S, Aitken CE, Korlach J, Flusberg BA, Turner SW, Puglisi JD (2010) Real-time tRNA transit on single translating ribosomes at codon resolution. Nature 464: 1012–1017

Uemura S, Dorywalska M, Lee TH, Kim HD, Puglisi JD, Chu S (2007) Peptide bond formation destabilizes Shine-Dalgarno interaction on the ribosome. Nature 446: 454–457

Unwin PN, Taddei C (1977) Packing of ribosomes in crystals from the lizard Lacerta sicula. J Mol Biol 114: 491–506

Vogel Z, Vogel T, Elson D, Zamir A (1970) Ribosome activation and the binding of dihydrostreptomycin: effect of polynucleotides and temperature on activation. J Mol Biol 54: 379–386

von Bohlen K, Makowski I, Hansen HA, Bartels H, Berkovitch-Yellin Z, Zaytzev-Bashan A, Meyer S, Paulke C, Franceschi F, Yonath A (1991) Characterization and preliminary attempts for derivatization of crystals of large ribosomal subunits from Haloarcula marismortui diffracting to 3 A resolution. J Mol Biol 222: 11–15

Voorhees RM, Weixlbaumer A, Loakes D, Kelley AC, Ramakrishnan V (2009) Insights into substrate stabilization from snapshots of the peptidyl transferase center of the intact 70S ribosome. Nat Struct Mol Biol 16: 528–533

Voss NR, Gerstein M, Steitz TA, Moore PB (2006) The geometry of the ribosomal polypeptide exit tunnel. J Mol Biol 360: 893–906

Walter P, Johnson AE (1994) Signal sequence recognition and protein targeting to the endoplasmic reticulum membrane. Annu Rev Cell Biol 10: 87–119

Watson JD (1963) Involvement of RNA in the synthesis of proteins. Science 140: 17–26

Weinger JS, Parnell KM, Dorner S, Green R, Strobel SA (2004) Substrate-assisted catalysis of peptide bond formation by the ribosome. Nat Struct Mol Biol 11: 1101–1106

Weixlbaumer A, Jin H, Neubauer C, Voorhees RM, Petry S, Kelley AC, Ramakrishnan V (2008) Insights into translational termination from the structure of RF2 bound to the ribosome. Science 322: 953–956

Wekselman I, Davidovich C, Agmon I, Zimmerman E, Rozenberg H, Bashan A, Berisio R, Yonath A (2008) Ribosome's

mode of function: myths, facts and recent results. J Pept Sci 15: 122–130

Wilson DN (2004) Antibiotics and the inhibition of ribosome function. In: Nierhaus KH, Wilson DN (eds) Protein synthesis and ribosome structure. Weinheim, Germany: Wiley-VCH, pp 449–527

Wilson DN, Schluenzen F, Harms JM, Yoshida T, Ohkubo T, Albrecht R, Buerger J, Kobayashi Y, Fucini P (2005) X-ray crystallography study on ribosome recycling: the mechanism of binding and action of RRF on the 50S ribosomal subunit. Embo J 24: 251–260

Wohlgemuth I, Beringer M, Rodnina MV (2006) Rapid peptide bond formation on isolated 50S ribosomal subunits. EMBO Rep 7: 699–703

Wohlgemuth I, Brenner S, Beringer M, Rodnina MV (2008) Modulation of the rate of peptidyl transfer on the ribosome by the nature of substrates. J Biol Chem 283: 32229–32235

Woolhead CA, Johnson AE, Bernstein HD (2006) Translation arrest requires two-way communication between a nascent polypeptide and the ribosome. Mol Cell 22: 587–598

Woolhead CA, McCormick PJ, Johnson AE (2004) Nascent membrane and secretory proteins differ in FRET-detected folding far inside the ribosome and in their exposure to ribosomal proteins. Cell 116: 725–736

Yarus M (2010) Life from an RNA world: The ancestor within. Harvard University Press

Yonath A (2003) Ribosomal tolerance and peptide bond formation. Biol Chem 384: 1411–1419

Yonath A (2005) Antibiotics targeting ribosomes: resistance, selectivity, synergism, and cellular regulation. Annu Rev Biochem 74: 649–679

Yonath A, Bartunik HD, Bartels KS, Wittmann HG (1984) Some X-ray diffraction patterns from single crystals of the large ribosomal subunit from Bacillus stearothermophilus. J Mol Biol 177: 201–206

Yonath A, Bashan A (2004) Ribosomal Crystallography: Initiation, Peptide Bond Formation, and Amino Acid Polymerization are Hampered by Antibiotics. Annu Rev Microbiol 58: 233–251

Yonath A, Glotz C, Gewitz HS, Bartels KS, von Bohlen K, Makowski I, Wittmann HG (1988) Characterization of crystals of small ribosomal subunits. J Mol Biol 203: 831–834

Yonath A, Khavitch G, Tesche B, Muessig J, Lorenz S, Erdmann VA, Wittmann HG (1982a) The nucleation of crystals of the large ribosomal subunits from Bacillus stearothermophilus. Biochem Int 5: 629–636

Yonath A, Leonard KR, Wittmann HG (1987) A tunnel in the large ribosomal subunit revealed by three-dimensional image reconstruction. Science 236: 813–816

Yonath A, Muessig J, Tesche B, Lorenz S, Erdmann VA, Wittmann HG (1980) Crystallization of the large ribosomal subunit from B. stearothermophilus. Biochem Int 1: 315–428

Yonath A, Mussig J, Wittmann HG (1982b) Parameters for crystal growth of ribosomal subunits. J Cell Biochem 19: 145–155

Yonath A, Wittmann HG (1988) Crystallographic and image reconstruction studies on ribosomal particles from bacterial sources. Methods Enzymol 164: 95–117

Youngman EM, Brunelle JL, Kochaniak AB, Green R (2004) The active site of the ribosome is composed of two layers of conserved nucleotides with distinct roles in peptide bond formation and peptide release. Cell 117: 589–599

Yusupov MM, Tischenko SV, Trakhanov SD, Riazantsev SN, Garber MB (1988) A new crystallin form of 30S ribosomal subunits from Thermus thermophilus. FEBS Lett 238: 113–115

Yusupov MM, Yusupova GZ, Baucom A, Lieberman K, Earnest TN, Cate JH, Noller HF (2001) Crystal structure of the ribosome at 5.5 A resolution. Science 292: 883–896

Yusupova G, Jenner L, Rees B, Moras D, Yusupov M (2006) Structural basis for messenger RNA movement on the ribosome. Nature 444: 391–394

Zamir A, Miskin R, Elson D (1971) Inactivation and reactivation of ribosomal subunits: amino acyl-transfer RNA binding activity of the 30s subunit of *Escherichia coli*. J Mol Biol 60: 347–364

Zarivach R, Bashan A, Berisio R, Harms J, Auerbach T, Schluenzen F, Bartels H, Baram D, Pyetan E, Sittner A, Amit M, Hansen HAS, Kessler M, Liebe C, Wolff A, Agmon I, Yonath A (2004) Functional aspects of ribosomal architecture: symmetry, chirality and regulation. J Phys Org Chem 17: 901–912

Zhang B, Cech TR (1997) Peptide bond formation by in vitro selected ribozymes. Nature 390: 96–100

Zimmerman E, Yonath A (2009) Biological implications of the ribosome's stunning stereochemistry. ChemBioChem 10: 63–72

Ziv G, Haran G, Thirumalai D (2005) Ribosome exit tunnel can entropically stabilize {alpha}-helices. Proc Natl Acad Sci USA 102: 18 956–18 961

Structural studies on decoding, termination and translocation in the bacterial ribosome

2

Venki Ramakrishnan

1. Introduction

With the determination of the atomic structures of the ribosomal subunits in 2000, focus has shifted in the last decade to the study of functional states of the ribosome with a view to helping elucidate the mechanisms underlying the various steps of translation. Some of these studies could be carried out using crystals of the ribosomal subunits, recognition of codon-anticodon pairing by the ribosome during decoding in the 30S subunit, or studies on peptidyl transferase intermediates in the 50S subunit. Others, such as the interaction of elongation or release factors with the ribosome require high-resolution crystal forms of the intact 70S ribosome. In this chapter, we review our studies on decoding using the 30S subunit, which could use crystals of the subunit that diffracted to high resolution. However, other functional studies such as those on elongation and termination required new crystal forms of the 70S ribosome that also diffracted to high-resolution.

The structure at 5.5 Å resolution of the entire 70S ribosome complexed with mRNA and tRNA (Yusupov et al., 2001) was a major achievement and the culmination of over a decade of work that began with the crystallization of the 70S ribosome and its 30S subunit from *Thermus thermophilus* (Trakhanov et al., 1987). However, the limitation of resolution inherent to this crystal form precluded detailed structural studies on functional states of the ribosome. Another significant landmark was the determination of the structure of the *E. coli* ribosome to 3.5 Å resolution (Schuwirth et al., 2005), although, to date, this crystal form has not been able to accommodate full-length tRNAs with mRNA or most factors, thus limiting its utility.

In this context, two new crystal forms of the bacterial 70S ribosome discovered in our laboratory have proved very useful. The first, an orthorhombic crystal form that diffracts to about 3 Å resolution (Selmer et al., 2006) was very useful in both our and several other laboratories for studies on termination (Laurberg et al., 2008, Weixlbaumer et al., 2008, Korostelev et al., 2008), recycling (Weixlbaumer et al., 2007), peptidyl transferase (Voorhees et al., 2009), various antibiotics (Stanley et al., 2010) and a factor involved in the formation of the first peptide bond (Blaha et al., 2009). However, this crystal form, like the other 70S crystal forms that preceded it (regardless of space group and species), has ribosomal protein L9 extending out from the body of the 50S subunit and interacting with a neighboring 30S subunit in the crystal lattice in such a way that it sterically occludes the binding site for translational GTPases. In our experience, the interaction is strong enough to displace even a stably bound EF-G or EF-Tu; thus the crystals containing L9 we obtained always lacked GTPase factors.

As a result, we decided to delete the portion of the gene coding for the C-terminus of L9 that protruded out from the body of the molecule. The resulting strain, MRC-MSAW1, gave crystals of ribosomes bound to EF-G (Gao et al., 2009) and EF-Tu (Schmeing et al., 2009). In both cases, L9 was not observed in the resulting structure, suggesting that the residual fragment of L9 is either too unstable and is degraded upon synthesis, or does not assemble onto 50S subunits. Nevertheless, this crystal form has paved the way for studies of GTPase factors bound to the ribosome.

We describe below our studies on decoding and other functional aspects of the ribosome, initially using the 30S subunit but subsequently with the two new crystal forms of the 70S ribosome described above. Our focus is on results obtained in our laboratory since our chapter in the last ribosome book (Brodersen et al., 2002) and is not intended to be a comprehensive description of the field.

2. Studies on decoding

The accuracy of translation is much greater than can be expected from the free-energy difference between correct and incorrect base pairs in codon-anticodon interactions (reviewed in Ogle and Ramakrishnan, 2005). The ribosome plays an active role in tRNA selection, and pre-steady-state kinetics showed that the binding of cognate but not near-cognate tRNA induces a conformational change in the ribosome that leads to the acceleration of GTP hydrolysis (reviewed in Rodnina and Wintermeyer, 2001).

2.1. Insights from studies on the 30S subunit

With the determination of the atomic structure of the 30S subunit, it became possible to try to understand decoding in structural terms. The first clue in this direction was the structure of the 30S subunit with paromomycin (Carter et al., 2000). Paromomycin was previously known to bind to an internal loop of 16S RNA in the decoding center (Fourmy et al., 1996). In the 30S subunit, paromomycin induced a change in the conformation of two universally conserved adenosines, A1492 and A1493, so that the bases were displaced from an internal loop of helix 44 in the decoding center and were in a position to interact directly with the codon-anticodon helix (Figures 1A and B; Carter et al., 2000). Subsequently, we determined the structure of the 30S subunit in complex with oligonucleotide mimics of the A-site mRNA codon and the anticodon stem-loop of tRNA (Figure 1C) (Ogle et al., 2001). The binding of cognate tRNA to the 30S subunit not only induced changes in the conformation of the two adenines that were displaced by paromomycin, but also that of G530 on the other side of the decoding center, so that all three bases made close interactions with the minor groove of the codon-anticodon helix (Figure 1C).

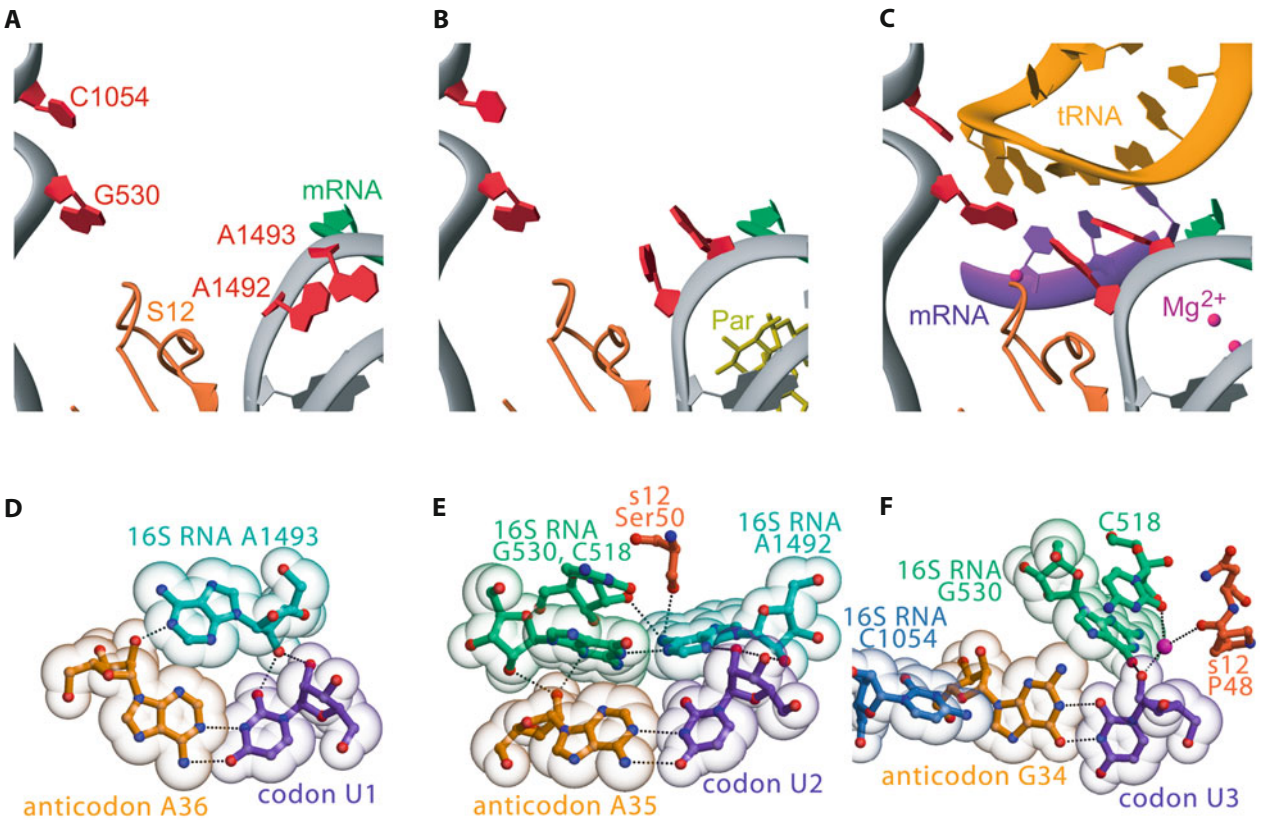

Fig. 1 Changes in the decoding center of the 30S subunit with the binding of paromomycin or tRNA. (A) The decoding center in the empty 30S subunit. (B) The decoding center in the presence of the antibiotic paromomycin. (C) The decoding center in the presence of oligonucleotide mimics of the mRNA codon and the tRNA anticodon stem-loop. (D, E) Interactions of the three ribosomal bases with the minor groove of the first, second and third base pairs respectively between the codon and anticodon. (Figure adapted from Ogle et al., 2001)

The shape of the minor groove was closely monitored at the first two positions (Figure 1D and E), but not at the third position (Figure 1F), where a GU wobble base pair was readily accommodated. Since the shape of the minor groove is invariant for all Watson-Crick base pairs, including the location of hydrogen-bonding acceptors at identical positions (Seeman et al., 1976), this allows the ribosome to monitor Watson-Crick base pairing at the first two positions while being more tolerant at the third position, thus offering a structural basis for the wobble hypothesis. The minor groove interactions also provide binding energy for cognate tRNA in excess of that for near-cognate tRNAs. The excess free energy has been estimated at 15–20 kJ/mole (Battle and Doudna, 2002), which by itself could explain the accuracy of decoding, except that, as predicted by kinetic data, the ribosome uses much of this binding energy to drive a conformational change that leads to GTP hydrolysis and tRNA selection rather than just to preferentially stabilize cognate tRNA (Pape et al., 1999).

The second consequence of tRNA binding appears to be a global conformational change in the 30S subunit (Ogle et al., 2001). A subsequent study with near-cognate tRNAs showed that although they bound to the 30S subunit with only slightly less affinity than cognate tRNA, they failed to induce this global conformational change unless the antibiotic paromomycin was also present (Ogle et al., 2002). This study provided a structural understanding of previous kinetic data that showed that paromomycin worked primarily by helping to accelerate GTP hydrolysis for near-cognate tRNAs rather than stabilizing their binding (Pape et al., 2000).

The global conformational changes induced in the 30S subunit involve a movement of the shoulder and platform domains relative to the rest of the 30S subunit (Figure 2). The movement would involve disruption or formation of contacts between the two domains in going from the empty (open) form to the tRNA-bound (closed) form. Interestingly, an analysis of a large body of biochemical and genetic data suggests that mutations such as the *ram* mutations in S4 and S5 that would make it easier to reach the closed form increase the error rate of the ribosome, while those such as the streptomycin resistance mutations in S12 that make it more difficult to reach the closed form result in lowering the error rate. The antibiotic streptomycin stabilizes the 30S subunit in a conformation similar to the closed form, thereby increasing error rates. This led to the proposal that the closed

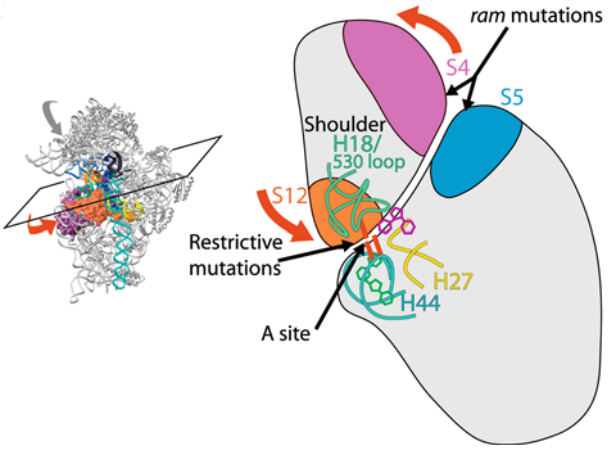

Fig. 2 Conformational changes and domain closure in the 30S ribosomal subunit effected by antibiotics or accuracy mutations of the ribosome. On the left is an overview of the 30S subunit showing the directions of the conformational changes in the domains. On the right is a schematic cross-section of the 30S subunit (as defined by the plane cutting the 30S subunit on the left), in the region of the decoding centre and proteins S4 (violet), S5 (blue) and S12 (orange). G530 and A1492/3 are represented by red bars; helices H44, H27 and H18 (with the G530-loop) are cyan, yellow and turquoise, respectively. The rotation of the shoulder domain (red arrows) during the transition to the closed 30S conformation disrupts an interface between S4 and S5, while the H18/530-loop/S12 region forms new contacts to H27 and H44. Mutations in these regions either increase or decrease mRNA misreading. Paromomycin (dark green rings) and streptomycin (dark pink rings) induce translational errors by facilitating domain closure. (Figure reproduced from Ogle et al., 2003)

form of the 30S subunit is required for tRNA selection (Ogle et al., 2002).

In conjunction with cryo-EM structures of EF-Tu bound to the ribosome (Stark et al., 1997) (Valle et al., 2002), it could be seen that domain closure upon codon recognition involved a movement of the shoulder domain of the 30S subunit towards the ternary complex of EF-Tu and tRNA. The tRNA in the cryo-EM structure was shown to be bent in the anticodon stem (Valle et al., 2002). This led to an integrated model for decoding which proposed that the additional energy from the interaction with the minor groove of the Watson-Crick codon-anticodon base pairs would be used to induce a domain closure in the 30S subunit that would be essential to reach the state required for GTP hydrolysis by EF-Tu (Ogle et al., 2002). After GTP hydrolysis and release of EF-Tu from the ribosome, the distorted tRNA would then relax into the peptidyl transferase center during accommodation.

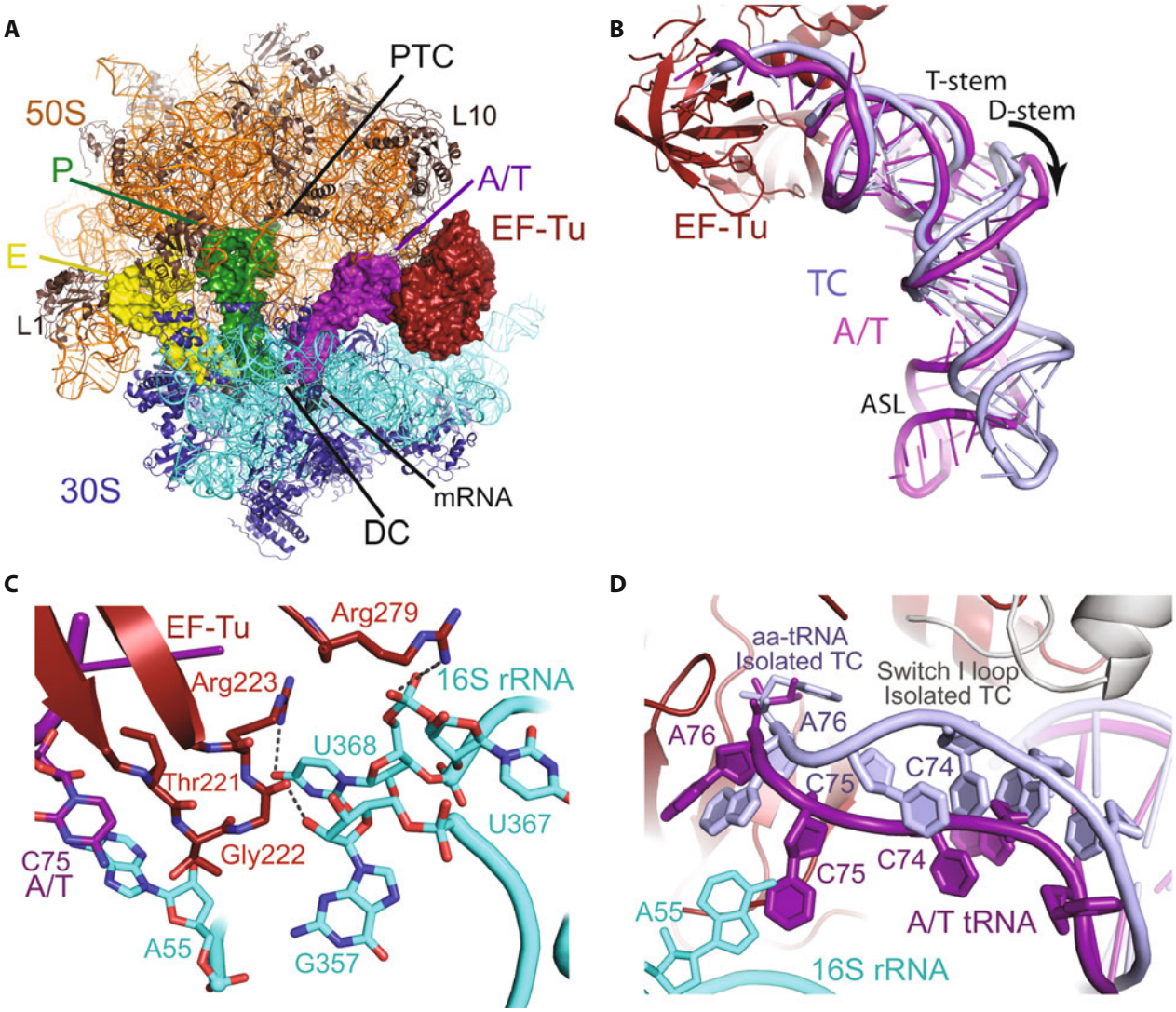

Fig. 3 The kirromycin-stalled complex of EF-Tu and aminoacyl tRNA with the ribosome. (A) Overview of the structure showing the three tRNAs and EF-Tu, the peptidyl transferase center (PTC) and the decoding center (DC). (B) Comparison of the ternary complex in the ribosome (purple) with that in isolation (slate blue), showing the distortion in the anticodon and D stems. (C) Detail showing how domain closure of the shoulder of the 30S subunit and a conformational change of a highly conserved loop of EF-Tu stabilize an interaction between EF-Tu and 16S RNA. (D) Detail showing how a stacking interaction between A55 of 16S RNA and C75 of tRNA stabilize a 3' end of tRNA that is displaced by as much as 6 Å relative to its conformation in the isolated ternary complex (gray). (Figure reproduced from Schmeing et al., 2009)

2.2. Structures of the ribosome with elongation factor Tu and aminoacyl tRNA

It became clear that despite increasingly higher resolution models of the EF-Tu-tRNA-ribosome complex determined by cryo-EM, the molecular details of decoding would require a high-resolution structure, currently reachable only by crystallography. Crystallization attempts of this complex over several years were unsuccessful. However, the L9-deletion mutant ribosomes described earlier were amenable to crystallization of GTPase factors with the ribosome (Gao et al., 2009) and were used to crystallize and solve the structure of a kirromycin-stalled complex of EF-Tu with aminoacyl-tRNA and the ribosome (Figure 3A) (Schmeing et al., 2009). Kirromycin prevents the large conformational change in EF-Tu between the GTP and GDP forms, thus trapping EF-Tu on the ribosome after GTP hydrolysis.

The detailed structure of the EF-Tu-tRNA-ribosome complex clarified many issues. The distortion in the tRNA was visible in detail and involved an untwist-

ing accompanied by a widening of the groove in the anticodon-stem as well as a movement of the D loop (Figure 3B). The movement of the shoulder domain of the 30S subunit predicted from earlier studies on the subunit structure was accompanied by a movement of a highly conserved loop in EF-Tu that would stabilize the conformation of EF-Tu on the ribosome (Figure 3C). A striking observation was that the 3' end of tRNA was pulled away by almost 6 Å compared to the structure of the ternary complex in the absence of the ribosome. This altered conformation was stabilized by a stacking interaction with a base in the 30S subunit (Figure 3D), and would disrupt interactions between the 3' end and the switch I helix, which was disordered in the structure.

The structure shed light on how codon recognition could lead to GTP hydrolysis on EF-Tu and thus influence tRNA selection. The energy from the minor-groove interactions of residues of the decoding center with the codon-anticodon helix was used to stabilize the ternary complex on the ribosome, which consisted of the distorted form of tRNA as well as changes in EF-Tu. The distortion at the 3' end of the tRNA would destabilize the switch I loop, which according to previous suggestions would lead to exposure of the gamma phosphate of GTP to water and subsequent hydrolysis. After phosphate release, the GDP form of EF-Tu would have a significantly altered conformation, resulting in loss of many of its contacts with the ribosome, leading to its release. After EF-Tu release, there would be nothing to stabilize the tRNA in the distorted form; however since it would still be bound tightly to the decoding center through its anticodon loop, its 3' end would relax into the peptidyl transferase center thus initiating peptidyl transfer.

Because the kirromycin-stalled structure represented the state after GTP hydrolysis, it did not reveal much about the detailed mechanism of catalysis. Indeed, the catalytic histidine was in the "inactive" conformation, facing away from the GDP and making an interaction with the sarcin-ricin loop (SRL). The role of the SRL in catalysis was unclear.

The mechanism of GTP hydrolysis has more recently been investigated by a structure of the EF-Tu-tRNA complex bound with a GTP analogue, GDPCP, in complex with the ribosome (Voorhees et al., 2010). This structure captures the catalytic histidine of EF-Tu in the activated form (Figure 4A), where it coordinates the catalytic water molecule that interacts with the gamma phosphate of GDPCP (Figure 4B, middle panel). The other nitrogen of the histidine interacts with the phosphate oxygen of A2662 of the SRL. This is precisely the nucleotide that is the target of the nuclease toxin α-sarcin. An unexpected observation is that switch I is not disordered in the structure even though the 3' end of tRNA is distorted as in the kirromycin-stalled complex. Thus loss of contacts with the 3' end of tRNA is not sufficient for switch I to become disordered. Also, it appears that the disordering of switch I to open a "hydrophobic gate" is not necessary for the repositioning of the catalytic histidine and water molecule as has been previously proposed (Vogeley et al., 2001) (Sengupta et al., 2008, Villa et al., 2009, Schuette et al., 2009) (Schmeing et al., 2009). Rather, subtle movements of elements of EF-Tu around the GTP (Figure 4A) may facilitate the positioning of His84 and the water to coordinate with the gamma phosphate. The role of the SRL appears to be to hold the catalytic histidine in the active conformation. Interestingly, the conformation of the SRL itself is essentially identical to that found in factor-free structures of the ribosome. The structure rationalizes the universal importance of the SRL and a common catalytic mechanism for all ribosomal GTPase factors. The difference in their action can be attributed to the differences in the conformation of the ribosome in various states, so that each state would allow only a particular factor to be positioned with the SRL in exactly the right position to activate the catalytic histidine.

3. Studies on termination

The three stop codons are decoded by the so-called "class-I" release factors. In bacteria, there are two factors, RF1 and RF2, which have overlapping specificity: RF1 recognizes UAG, RF2 recognizes UGA, whereas both recognize UAA. The high-resolution crystal form of the 70S ribosome (Selmer et al., 2006) made it possible to obtain high-resolution structures of the ribosome complexed with either RF1 (Laurberg et al., 2008) or RF2 (Weixlbaumer et al., 2008, Korostelev et al., 2008, Korostelev et al., 2010). Taken together, these structures provided a structural basis for understanding the specificity of stop-codon recognition by RF1 and RF2. However, the structures did not make it entirely clear why the substitution of a tripeptide motif would switch the specificity of RF1 and RF2 (Ito et al., 2000), nor why a single mutation at a location that did not interact directly with the stop codon would cause a release factor to read all three stop codons (Ito et al., 1998). Thus although the basis of specificity is much better understood, more work is still required.